BIREFRINGENT INTERFEROMETER DIFFUSION

MEASUREMENTS IN THE URANYL

NITRATE-WATER SYSTEM

By

WILLIAM PATRICK METZ

Bachelor of Science

Iowa State University of

Science and Technology

Ames, Iowa

1967

Submitted to the Faculty of the
Graduate College of the
Oklahoma State University
in partial fulfillment of
the requirements for
the Degree of
MASTER OF SCIENCE
May, 1969

BIREFRINGENT INTERFEROMETER DIFFUSION

MEASUREMENTS IN THE URANYL

NITRATE-WATER SYSTEM

Thesis Approved:

_____
Thesis Adviser

_____

_____
Dean of the Graduate College

724992

ii

PREFACE

Molecular diffusion properties have been of interest for many years. Recently, optical techniques have been developed to observe these properties under conditions suitable for mathematical modeling of the diffusion process.

The object of this study is to observe diffusion phenomenon in a binary system, to compare these data with ionic solution theory and to do preliminary work for a more extensive study of multicomponent systems using a birefringent system.

TABLE OF CONTENTS

LIST OF TABLES

LIST OF FIGURES

LIST OF PLATES

CHAPTER I

INTRODUCTION

The measurement of diffusion coefficients is one of the most difficult tasks facing the experimentalist. Several methods have been developed over the years to measure the diffusion coefficient by observing the diffusion process. These methods can be conveniently classified as restricted or unrestricted diffusion processes.

Restricted diffusion processes were the first type of processes used to study diffusion. Almost all early measurements on these processes were made by "layer analysis," which was described by Graham (13). Later, the steady state methods were developed where diffusion was allowed to occur in such a way that a time-invariant system resulted.

Presently, free diffusion or unrestricted processes have come into popularity. In this type of system, unrestricted diffusion takes place from an initially sharp boundary.

Several optical techniques have been developed to observe free diffusion. Generally, optical techniques involve the formation of constructive and destructive interference patterns. Some common optical interferometers are Gouy (12), Rayleigh (21), and Mach-Zehnder (21).

The prime advantage of optical techniques is that the diffusion coefficient can be measured using very small concentration gradients.

The diffusion coefficient for many electrolytes is a function of concentration. When the diffusion coefficient can be measured using a very small concentration gradient, the effect of concentration on the diffusion coefficient can be neglected, and differential diffusion coefficient can be measured directly. The use of small concentration gradients also enables the experimenter to measure diffusion coefficients in very dilute solutions.

In 1957, Olaf Bryngdahl (3) published a new optical method for diffusion studies. The method utilizes birefringent interference and produces a fringe pair pattern that can readily be modeled in diffusion experiments. This optical method, Bryngdahl's "first" interferometer, was the method used in this work to measure binary diffusion coefficients.

Later in 1960, Bryngdahl and Ljunggren (5) announced a modification to Bryngdahl's first interferometer. This "second" interferometer produces a refractive index gradient record. Bryngdahl's second interferometer also utilized birefringent interference. Bryngdahl's second interferometer was used in the ternary study. The data used to analyze models for calculating diffusion coefficients was obtained using Bryngdahl's second interferometer.

The purpose of this work was to use the birefringent interferometer to study the uranyl nitrate-water system diffusion characteristics in dilute solution and to compare these data with data from other experimental methods and with theory for diffusion in dilute solutions. Several techniques for calculating the diffusion coefficient from birefringent data were studied. A qualitative study of

diffusion in the ternary system of uranyl nitrate-nitric acid-water was made.

CHAPTER II

THEORY

In 1855, the mass transport process of diffusion was compared to conductive heat transfer by Fick, who introduced the equation

$$J = -D(dC/dx) \qquad (2\text{-}1)$$

for one-directional diffusion. J is a flux vector and dC/dx is the mass driving force in the x direction with D as the proportionality constant, termed the diffusion coefficient. Equation (2-1) is known as Fick's First Law.

Recognizing the law of mass conservation in a closed system and assuming no volume change in mixing, the time variant form of Equation (2-1) may be written for one-dimensional diffusion as

$$\frac{\partial C}{\partial t} = \frac{\partial}{\partial x}\left(D\,\frac{\partial C}{\partial x}\right) \qquad (2\text{-}2)$$

Equation (2-2) is known as Fick's Second Law. If, for convenience, the diffusion coefficient is assumed not to vary with concentration, Equation (2-2) becomes

$$\frac{\partial C}{\partial t} = D\,\frac{\partial^2 C}{\partial x^2} \qquad (2\text{-}3)$$

In order to solve Equation (2-3), the boundary conditions of a specific system must be used. For diffusion due to an initial step

boundary in a system with no bounds in the direction of diffusion, the following boundary conditions may be written:

$$t \leq 0 \qquad C = C_1 \qquad x < 0 \qquad (2\text{-}4a)$$

$$t \leq 0 \qquad C = C_2 \qquad x > 0 \qquad (2\text{-}4b)$$

$$\text{all} \quad t \qquad C = C_1 \qquad x \rightarrow -\infty \qquad (2\text{-}5a)$$

$$\text{all} \quad t \qquad C = C_2 \qquad x \rightarrow +\infty \qquad (2\text{-}5b)$$

Letting

$$y = x/\sqrt{t} \qquad (2\text{-}6)$$

The first integration, after integration constant evaluation, gives

$$\frac{\partial C}{\partial x} = \frac{(C_2 - C_1)}{\sqrt{4\pi Dt}} \ \exp\left(\frac{-x^2}{4Dt}\right) \qquad (2\text{-}7)$$

Integrating again yields

$$C - \bar{C} = \frac{(C_2 - C_1)}{2} \ \text{erf}\left(\sqrt{\frac{1}{4Dt}} \ x\right) \qquad (2\text{-}8)$$

where $\bar{C} = (C_1 + C_2)/2$.

Bryngdahl's First Interferometer

In 1957, Olaf Bryngdahl (3) published a new interferometric method utilizing birefringence for diffusion measurements. The optical arrangement for this interferometer is shown schematically in Figure 1a. The system consists of a horizontal slit, E, illuminated by monochromatic light; collimating lenses L_1 and L_2; polarizers P_1 and P_2; focusing lens L_3; Savart plate S; the diffusion cell; and the image plane M.

The resulting image in plane M consists of an even number of symmetric fringes. Each fringe is a distance x from the initial position of the interface. For a corresponding fringe pair, the fringes are a distance 2x apart. Since the fringes are a result of a refractive index change in the diffusion cell and the refractive index of a diffusing solution varies with time (3), the variation of the 2x distance of a definite fringe pair can be observed with time.

Bryngdahl proceeded from Equation (2-8) to derive an expression that described the fringe pair separation, 2x, as a function of time:

$$(2x)^2 = 8Dt \left(1 + \ln \frac{t_i}{t} \right) \tag{2-9}$$

where t_i is the time of greatest separation of the fringe pairs of interest.

Equation (2-9) can be modified by defining t_1 and t_2 as the respective times that the fringe pair of interest are separated by a given distance $(2x)^2$. After solving for D, this modification results in the two-point equation (3)

$$D = \frac{(2x)^2 \left(\frac{1}{t_1} - \frac{1}{t_2} \right)}{8 \ln t_2/t_1} \tag{2-10}$$

Equations (2-9) and (2-10) can be used to evaluate the diffusion coefficient from birefringent data from Bryngdahl's first interferometer.

Bryngdahl's Second Interferometer

Bryngdahl's (5) second interferometer is shown schematically in

a. Bryngdahl's First Interferometer

E   P₁   L₁ Cell L₂   L₃   S₁   P₂   M

b. Bryngdahl's Second Interferometer

E   P₁   L₁   Cell   L₂   L₃ P₂ S₁   L₄   S₂   P₃   M
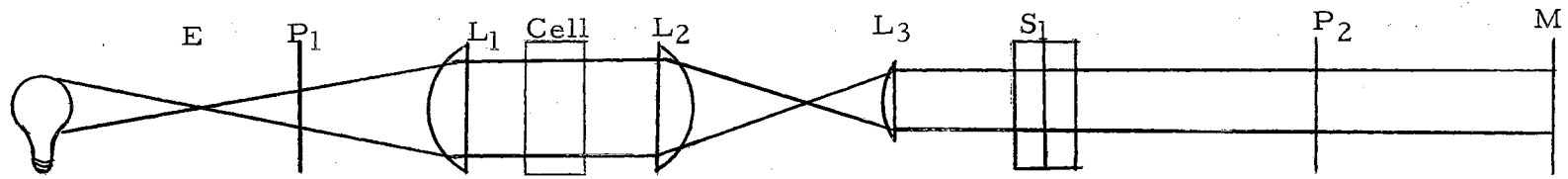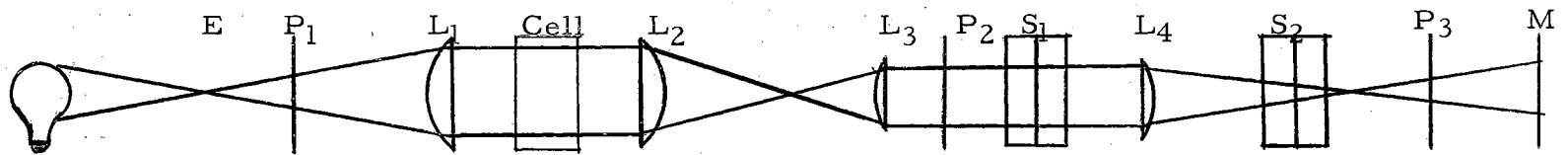
Figure 1.   Bryngdahl's Optical Arrangements

Figure 1b. The system consists of: a slit source of monochromic light E; collimating lenses L_1 and L_3; converging lenses L_2 and L_4; polarizers P_1, P_2, and P_3; Savart plates S_1 and S_2; the cell; and the image plane M. The resulting image is a direct plot of the refractive index gradient curve in the cell.

The refractive index of a binary dilute electrolyte solution can be approximated by the truncated series

$$n_{tol} = n_{sol} + R_1 C_1 \tag{2-11}$$

where n_{tol} is the solution refractive index, n_{sol} is the solvent refractive index, and R_1 is the refractive index increment of solute 1 of concentration C_1.

Substituting Equation (2-11) into Equation (2-7) gives

$$\frac{\partial n_{tol}}{\partial x} = \frac{\Delta n_{tol}}{\sqrt{4\pi Dt}} \exp\left(\frac{-x^2}{4Dt}\right) \tag{2-12}$$

Δn_{tol} is the total refractive index change across the diffusing boundary.

Equation (2-12) can be solved for the diffusion coefficient by several techniques. Skinner (22) has summarized the two-point method along with the corresponding time corrections involved to correct for nonideal initial conditions in the cell.

The solution of Equation (2-12) involving two points is

$$D = \frac{x_2^2 - x_1^2}{4t \ln\left(\frac{H_1}{H_2}\right)} \tag{2-13}$$

where H_i is the height of the refractive index gradient curve at a distance x_i from the center of that curve at time t.

The diffusion cell used in this study was a flowing-junction cell patterned after one utilized by Dr. H. Svensson. Diffusion cell characteristics have been reviewed by Bryngdahl (4), who recommended the flowing-junction cell. In this type of cell the initially sharp boundary is formed by allowing the solution to flow together into a narrow horizontal slit in the side wall of the diffusion cell.

In a flowing-junction cell, the infinitely thin interface boundary condition, Equations (2-4a) and (2-4b), must be corrected because of the finite thickness of the initial interface. Others (3) (27) have assumed that the finite width interface is equivalent to diffusion from a step interface for a short time period, ΔT. This correction is made by adding a ΔT time correction to all the time measurements. Thus, adding the time correction, ΔT, to the time variable, t, in Equation (2-13) and writing the resulting equation for two measured times, t_1 and t_2, the time corrected diffusion coefficient, D^t, can be calculated. The resulting equation is

$$D^t = \frac{1}{t_1 - t_2} (D_1 t_1 - D_2 t_2) \qquad (2\text{-}14)$$

The four-point method can easily be deduced by writing Equation (2-13) twice and adding an arbitrary constant, α, to each value of x_i. The solution is

$$D = \frac{(x_2'^2 - x_1'^2) - B(x_4'^2 - x_3'^2)}{4t (\Theta_{12} - \Theta_{34} B)} \qquad (2\text{-}15)$$

where

$$B = \frac{x_1^{\bullet} - x_2^{\bullet}}{x_3^{\bullet} - x_4^{\circ}} \qquad (2\text{-}16)$$

$$\Theta_{ij} = \ln\left(\frac{H_i}{H_j}\right) \qquad (2\text{-}17)$$

$$x_i^{\bullet} = \alpha + x_i \qquad (2\text{-}18)$$

The advantage of Equation (2-15) is that the centroid coordinate of the refractive index gradient curve need not be determined.

Since Equation (2-12) is of Gaussian form, a method of area-moment evaluation can be used. Bevilacqua (2) has discussed this method at length. The diffusion coefficient expression is

$$D = \left[\frac{\sum s_i^2 H_i}{\sum H_i} - \left(\frac{\sum s_i H_i}{\sum H_i}\right)^2\right] \frac{\omega^2}{2t} \qquad (2\text{-}19)$$

where H_i is the height of the refractive index gradient curve from an approximated centroid, s_i is an integer, and ω is a scaling constant.

Multicomponent Systems

Free diffusion in multicomponent systems with interacting flow has been modeled and solved by Fugita and Gosting (11) for a three-component system. The equations describing one-dimensional diffusion in such a system are deduced from Fick's Second Law and are

$$\frac{\partial c_1}{\partial t} = D_{11} \frac{\partial^2 c_1}{\partial x^2} + D_{12} \frac{\partial^2 c_2}{\partial x^2} \tag{2-20}$$

$$\frac{\partial c_2}{\partial t} = D_{21} \frac{\partial^2 c_1}{\partial x^2} + D_{22} \frac{\partial^2 c_2}{\partial x^2} \tag{2-21}$$

where C_i is the concentration of the ith component and is a function of time (t) and location (x), and D_{ij} is the proportionality constant or diffusion coefficient term for the movement of the ith component due to the jth driving force in the given system.

The equations are solved by compounding variables, letting

$$y = x/2 \sqrt{t} \tag{2-22}$$

The boundary conditions are, for $i = 1, 2,$

$$c_i = \overline{c}_i - \Delta c_i/2 \text{ for } x > 0, \ t \leq 0 \tag{2-23}$$

$$c_i = \overline{c}_i + \Delta c_i/2 \text{ for } x < 0, \ t \leq 0 \tag{2-24}$$

$$c_i \rightarrow \overline{c}_i + \Delta c_i/2 \text{ for } x \rightarrow -\infty, \ t > 0 \tag{2-25}$$

$$c_i \rightarrow \overline{c}_i - \Delta c_i/2 \text{ for } x \rightarrow \infty, \ t > 0 \tag{2-26}$$

where

$$\overline{c}_i = \left[(c_i)_A + (c_i)_B \right] /2 \tag{2-27}$$

$$\Delta c_i = (c_i)_B - (c_i)_A \tag{2-28}$$

A and B denote the solutions above and below the $x = 0$ plane, respectively. Conditions (2-23) and (2-24) constitute the infinitely

thin interface assumption.

The exact solution of Equation (2-20) and (2-21) for solute con-centrations (i denoting the component of interest, and j denoting the other component) is

$$c_i = \bar{c}_i + K_i^+ \, \psi \, (\sqrt{\sigma}_+ \, y) + K_i^- \, \psi \, (\sqrt{\sigma}_- \, y) \qquad (2\text{-}29)$$

where

$$\psi(q) = \text{erf}(q) = \frac{2}{\sqrt{\pi}} \int_0^q e^{-q^2} dq \qquad (2\text{-}30)$$

$$K_i^{\pm} = \frac{\left\{ (D_{jj}-D_{ii}) \pm \left[(D_{jj}-D_{ii})^2 + 4D_{ii}D_{ii} \right]^{1/2} \right\} \Delta c_i - 2D_{ij} \, \Delta c_j}{4 \left[(D_{jj}-D_{ii})^2 + 4D_{ij}D_{ji} \right]^{1/2}} \qquad (2\text{-}31)$$

$$\sigma^{\pm} = \frac{1}{2} \left\{ \frac{(D_{jj} + D_{ii}) \pm \left[(D_{jj}-D_{ii})^2 + 4D_{ij}D_{ji} \right]^{1/2}}{D_{ii}D_{jj} - D_{ij}D_{ji}} \right\} \qquad (2\text{-}32)$$

From this solution, several methods of evaluating the diffusion coefficients for Gouy fringe deviation graphs have been used. The most common of these methods are the reduced second-and fourth-moment method and the reduced height-area ratios and second-moment method (11). The major drawbacks of these methods are the large volume of data required for measurements and their applicability only to single-peaked systems.

Solution Theory for Diffusion Measurements

Solutions of electrolytes are very nonideal, and methods of

predicting the diffusion coefficient as a function of concentration are usually inadequate. However, some basic theories for diffusion in solutions have been developed. These theories are of interest in observing the deviation of data and theory in very nonideal electrolyte solutions.

The Nernst-Hartley Relation

Nernst and Hartley (21) recognized that the proper driving force for diffusion is the chemical potential gradient and not the concentration gradient as Fick proposed. They also related the dilute solution diffusion properties of an electrolyte to ionic transport numbers and ionic activity.

The Nernst-Hartley relation is

$$D = D^O \left(1 + C \frac{d \ln \gamma_{\pm}}{d C} \right) \qquad (2\text{-}33)$$

where D^O is the Nernst limiting value of the diffusion coefficient and is

$$D^O = \frac{RT(\nu_1 + \nu_2)}{F^2 \nu_1 |z_1|} \frac{\lambda_1^o \lambda_2^o}{(\lambda_1^o + \lambda_2^o)} \qquad (2\text{-}34)$$

The reader is referred to Appendix C for sample calculations in the $UO_2(NO_3)_2\text{-}H_2O$ system.

Thus, if the measured diffusion data are corrected by a thermodynamic correction factor, φ, where

$$\varphi = \left(1 + C \frac{d \ln \gamma_{\pm}}{d C} \right) \qquad (2\text{-}35)$$

the resulting values of the diffusivity will be constant and equal to the Nernst limiting value. Any deviation of real solution diffusivity from the Nernst limiting value may be attributed to the nonideality in thermodynamic solution behavior, which is allowed for by the factor φ (21).

Onsager-Fuoss

Onsager and Fuoss (21) evaluated the electrophoretic contribution to diffusion, the effect of electrical neutrality in the solution during the diffusion process, in terms of velocity of the ions and their absolute mobilities. Harned and Owen (21) obtained a limiting equation for the diffusion coefficient of a salt. This limiting equation is

$$D = D_o - \mathcal{S}_{(D)} \sqrt{C} \qquad (2\text{-}36)$$

where D_o is the Nernst limiting value.

Thus, the diffusion coefficient of an electrolyte is a linear function with respect to the square root of concentration. This theory is applicable only in very dilute solutions; that is, as the solute concentration goes to zero.

Sample calculations are presented in Appendix C for evaluation of Equation (2-36) in the $UO_2(NO_3)_2$-H_2O system.

Wishaw Diffusion Theory

The Wishaw-Stokes (28) theory accounts for some of the nonidealities in associated, hydrated, multi-ion electrolyte solution. They have proposed that diffusivities in associated solutions be

represented by

$$D = (1 + C \frac{\partial \ln \gamma}{\partial C})(1 - 0.01\ C\ h)\left[1 + 0.018\ C\left(\frac{2D^*_{H_2O} - h}{D_0}\right)\right]$$

$$X\ \left[\alpha(D_0 + \Delta_1 + \Delta_2) + 2(1 - \alpha)D_{12}\right]\left(\frac{\eta_0}{\eta}\right) \qquad (2\text{-}37)$$

where: $\left(1 + C \frac{\partial \ln \gamma}{\partial C}\right)$ is the thermodynamic correction factor;

$(1 - 0.01\ C\ h)$ corrects for hydration effects; $\left[1 + 0.018\ C\left(\frac{2D^*_{H_2O} - h}{D_0}\right)\right]$

is a solvent correction factor; $\left[\alpha(D_0 + \Delta_1 + \Delta_2) + 2(1 - \alpha)D_{12}\right]$

is an electrophoretic correction; and $\left(\frac{\eta_0}{\eta}\right)$ is a viscosity correction.

The Wishaw-Stokes theory is applicable to the saturated solution conditions.

Appendix B contains the computer program for evaluation of the Wishaw-Stokes expression for the $UO_2(NO_3)_2$-H_2O system.

The Wishaw-Stokes theory can be applied at any concentration and is of interest in estimating the variation of diffusion data with concentration. The Nernst and Onsager theories are applicable in very dilute solutions and have been shown (21) to be qualitatively adequate in describing diffusion in very dilute solutions.

CHAPTER III

APPARATUS

A birefringent interferometer of Bryngdahl's first type was used in the binary diffusion measurements. The interferometer is shown schematically in Figure 2a. The diffusion observations in the three-component system were made using Bryngdahl's second type of interferometer, shown in Figure 2b.

The interferometers were similar to those described by Bryngdahl (3) (5). The light source used was a Spectra-Physics helium-neon gas laser, Model 130. Lenses L_1 and L_2 were diverging and collimating lenses, respectively. Two flowing-junction cells were used in this study. A cell 3 mm wide, 50 mm deep and 70 mm high was used in Bryngdahl's first type of interferometer in this study. A cell 25 mm wide, 50 mm deep and about 70 mm high was used in Bryngdahl's second type of interferometer in this study. Savart plates S_1 and S_2, polarizers P_1 and P_2, focusing lense L_3, and a camera completed the optical arrangements used. For a detailed description of the optical equipment and alignment techniques, diffusion cell, and temperature control systems, the reader is referred to the work of Skinner (22) and Slater (23).

A 35 mm Nikon Model F camera with Kodak High Contrast Copy film was used to photograph the fringe patterns.

All film measurements were made on a Vanguard Motion Analyzer,

16

a. Bryngdahl's First Interferometer

Laser L_1 L_2 Cell S_1 P_1 L_3 Camera

b. Bryngdahl's Second Interferometer

Laser L_1 L_2 Cell S_1 P_1 L_3 S_2 P_2 Camera
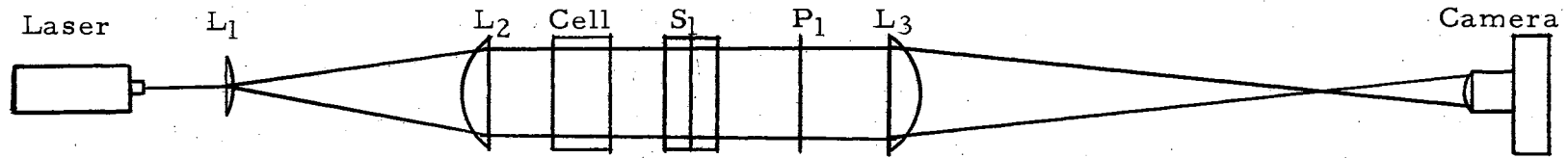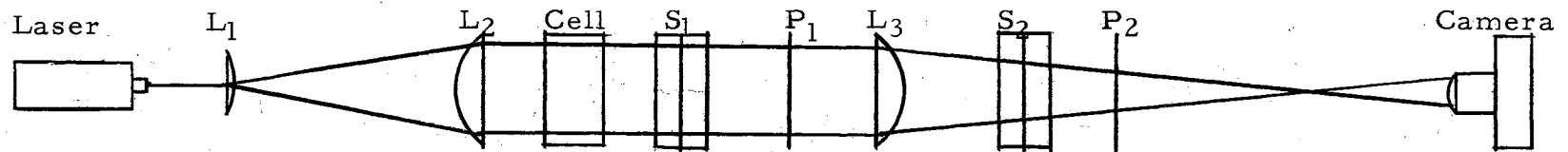
Figure 2. Optical Arrangement For This Study

Model M7-3-1, from the Vanguard Instrument Corporation. The Vanguard

Motion Analyzer has an image magnification of about 17 and is cali-

brated to 1/1000 inch.

Three methods were used for solution analysis. For uranyl

nitrate-water solutions in the range of 0.01-2.0 molar, a Precision

Refractometer, Number 33-45-03-01, from Bausch and Lomb, Inc., was

used. Slater's (23) refractive index data were used for calibration.

The data are presented in Appendix A, with the results of a linear

least squares analysis.

For uranyl nitrate-water solutions below 0.01 molar, a Beckman

Instruments, Inc., Model 2400 DU Spectrophotometer was used for

solution analysis. A detailed description of this analytical method

is given by Slater (24). Results of the calibration can be found in

Appendix A and agree with those found by Slater.

Uranyl nitrate-nitric acid-water solutions concentrations were

measured by a conductiometric titration method, based on the work of

Mundy (17). A more detailed description of this technique is avail-

able in Appendix D.

CHAPTER IV

EXPERIMENTAL PROCEDURE

The procedure followed in obtaining data for this study falls
conveniently into four divisions. These divisions are: (a) pre-
paring the solutions, (b) filling the cell, (c) taking photographs of
the fringe patterns, and (d) collecting data from the photographs. A
detailed explanation of each step is presented in the following
paragraphs.

Preparing the Solutions

Uranyl nitrate solutions were prepared in two ways: (a) by
weighing appropriate amounts of uranyl nitrate hexahydrate crystals
using a Mettler Model B6 balance, dissolving the crystals, and dilu-
ting to a known solution volume with distilled water; and (b) by
analyzing a solution and diluting to desired concentration. In all
cases, calibrated volumetric flasks and pipettes were used for volu-
metric measurements.

Two liters of the more dense solution were made, and one-half of
this solution was diluted to obtain the less dense solution. The
amount of diluting distilled water was calculated from Equation (4-1),

$$\Delta V = \frac{V_H \Delta c}{c_L}$$

(4-1)

where ΔV is the volume of dilution water, V_H is the volume of the more dense solution being used for dilution, C_L is the concentration of the less dense solution, and ΔC is the desired concentration difference.

Filling the Cell

The more dense solution was fed into the bottom of the cell until the entrance and exit lines were filled. The less dense solution was then fed slowly into the cell from the top, while the more dense solution was allowed to flow back into the reservoir flask. The replacement of the more dense solution by the less dense solution in the top section of the cell and the upper entrance line was done by giving the less dense solution reservoir a higher head than the more dense solution head. The solution heads were then allowed to equilibrate.

The exit valves were opened to allow a 60 drops per minute flow rate from each exit slit. This rate was continued until an interface could be seen in the camera viewfinder. The flow rate was then slowed to about 30 drops per minute per exit slit for about 15 minutes. Flow was then stopped and the diffusion process was observed for a few minutes before the slower flow rate was resumed. This observation was made to determine when the solution heads were precisely the same.

The solution heads were assumed equal if the interface did not move when the exit flow was stopped. Equalizing the solution heads required about one hour or more of draw-off time.

The interface was formed using a draw-off rate of 30 ± 1 drops per minute per exit slit. Exit flow at this rate was continued for at

least 15 minutes and until the interface was thin and distinct when observed through the camera viewfinder.

Photographing of Fringe Pattern

When the interface was steady and sharp, the draw-off rate was stopped, and fringe movements were observed to get an estimate of the rate at which the fringe movements occurred. Photographs were taken over a ten minute diffusing time for a concentration gradient of 0.02 molar in the binary uranyl nitrate system. Approximately thirty to forty photographs were taken at 15 second intervals during the first five minutes of diffusion and at 30 second intervals for the remainder of the diffusion time.

Replicate runs were made by reforming the interface and repeating the photographing procedures. Three consecutive replicates were made at each concentration of interest.

Data Collection

The system magnification for the optical arrangement and the Vanguard Motion Analyzer was measured by photographing a transparent reproduction of graph paper. The transparent reproduction of graph paper was placed in a position corresponding to one-third the way through the cell. However, it was found that such measurements varied significantly, and magnification was set by using the magnification value which gave the value of 14.75×10^{-6} cm^2/sec for $\bar{C}$ = .25 M NaCl solution (21).

All film measurements were made on the Vanguard Motion Analyzer. Measurements of a binary uranyl nitrate-water replicate run were made

by using a randomized complete block design with three blocks and one

observation per treatment.

CHAPTER V

RESULTS AND DISCUSSION

The results of this study are presented in three sections:
(a) evaluation of methods used to analyze birefringent data, (b) presentation of $UO_2(NO_3)_2$-H_2O diffusion data with comparison to other data from the literature and to ionic diffusion theories, and (c) the qualitative study of diffusion in $UO_2(NO_3)_2$-HNO_3-H_2O system.

Methods for Birefringent Data Analysis

In order to take satisfactory binary diffusion data, a complete study of analytical methods for evaluating birefringent diffusion data had to be made. The study was necessary to determine which mathematical model and which analytical method gave the best results.

For this study, the aqueous sodium chloride system was chosen as the standard for calibration and was used to obtain birefringent data which was needed to study different data analytical techniques. The sodium chloride system was chosen because the diffusion coefficient is known precisely. This study was made at an average sodium chloride concentration of 0.25 molar with a concentration gradient of 0.10 molar. These conditions were chosen because the diffusion coefficient of NaCl in this concentration range does not vary with concentration, and has an accepted value of $14.75 \times 10^{-5} cm^2 sec^{-1}$ (21).

Standard runs for both types of Bryngdahl's interferometers were

24

made. The results of these runs and of analytical methods used to evaluate the diffusion coefficients of these runs are discussed below.

Analytical Methods For Bryngdahl's First

Type of Interferometer

Several runs were made using Bryngdahl's first type of interferometer and a sodium chloride solution at an average concentration of 0.25 molar. These birefringent data were evaluated using three techniques. The basis of these techniques is the modeling equation derived by Bryngdahl (3) and presented in Chapter II, Equation (2-9). The equation is

$$y = 8B_1(t + B_2)\left(1.0 + \ln \frac{B_3 + B_2}{t + B_2}\right) \qquad (5\text{-}1)$$

where

$$y = (2x)^2 \text{ in cm}^2$$

$$B_1 = D \text{ in cm}^2/\text{sec}$$

$$B_2 = \Delta t \text{ in seconds}$$

$$B_3 = t_i, \text{ time of maximum value of } (2x)^2$$

$$t = \text{time in seconds}$$

A nonlinear curve-fitting program (9) using the Marquardt (16) technique was used to fit fringe pair distance measurements, (2x), as a function of time, t, for the three parameters, D, Δt, and t_i. This method gave a reproducibility in D of 0.75 per cent. There was a slight lack of fit between the data and the model in the early times during the diffusion run. This lack of fit is due to the inadequacies of the Δt time correction (23).

A method of iterating on Δt and fitting for the diffusion co-efficient and the time of maximum value of $(2x)^2$, using the nonlinear program, was used. Because of a nonlinear effect in the D versus $(2x)^2$ graph, an optimum Δt could not be determined and there was a definite lack of fit between the data and the model.

Thomas and Nicholl (27) used a linear form of Equation (5-1) to evaluate their data. A computer program was written to evaluate data using this method. The results showed no improvement in data analysis and there was a definite lack of fit between the data and the model.

The results of the model analysis showed that the nonlinear re-gression on Equation (5-1) gave the smallest error. As is shown in Appendix C, the error in the diffusion coefficient measurement is almost entirely due to fringe pair measurement error.

Analytical Methods For Bryngdahl's Second
Type of Interferometer

Several runs were made using Bryngdahl's second type of inter-ferometer using a sodium chloride solution at an average molar con-centration of 0.25. These birefringent data were evaluated using eleven techniques.

The two-point and four-point methods mentioned in Chapter II were used in evaluating the NaCl birefringent data. These methods did not give satisfactory, i.e., less than five per cent, results either in precision or accuracy.

To improve the precision of these methods, many $\left(\frac{\partial n}{\partial x} , x \right)$ data points were taken from a given fringe. All possible combinations of these data points were utilized in calculating the diffusion

coefficient by the two-point and four-point equations. Average values of the diffusion coefficient were than determined from both the two-point and four-point values. However, the results of these calculations did not significantly increase the precision of the diffusion coefficient measurement.

The equations for the two-point and four-point methods were linearized (see Appendix C). Sixteen $\left(\frac{\partial n}{\partial x}, x\right)$ points were taken, permuted, and fit by a linear regression. The results of this regression showed no increase in precision. Therefore, these evaluation methods were discarded. Poor precision was attributed to the error magnification due to the form of the equation.

The first integration of Fick's Second Law, Equation (2-7), was linearized in the form

$$\ln \frac{\partial n}{\partial x} = \ln \frac{\Delta n}{\sqrt{4\pi Dt}} - \frac{1}{4Dt}\left[x^2\right] \qquad (5-2)$$

The slope of the regression line was $\frac{-1}{4Dt}$, and the intercept value was $\ln \frac{\Delta n}{4\pi Dt}$. The result of this regression was a reproducibility in the order of ten per cent in the diffusion coefficient. Poor reproducibility was attributed to error in locating the centroid of the $\frac{\partial n}{\partial x}$ versus x graph which was used in x measurements.

The area-moment method, presented by Bevilacqua (2), was computerized. Appendix B contains the computer program. Appendix C has a summary of the method used and a presentation of the computer results.

The area-moment method gave the best precision in D, in the order of one to two per cent, of the previous methods discussed.

A nonlinear curve-fitting program (9) using the Marquardt (16) technique was used to fit $\frac{\partial n}{\partial x}$ and x data to evaluate two models.

The first model was a modification of Equation (2-12). The model was:

$$y = B_1 e^{-B_3(x-B_2)^2}$$ (5-3)

where

$$y = \frac{\partial n}{\partial x}$$

$$B_1 = \frac{\Delta n}{\sqrt{4\pi Dt}}$$

$$B_2 = \text{centroid coordinate}$$

$$B_3 = \frac{1}{4Dt}$$

The second model was a skewed form of Equation (5-3). The model was:

$$y = \frac{B_1 e^{-B_3(x-B_2)^2}}{1 + B_4 x}$$ (5-4)

where y, B_1, B_2, and B_3 are defined as above and B_4 is a skewed coefficient.

The results of this work are contained in Appendix C. Although the precision of these methods was an improvement over previously mentioned methods, the model showed a definite lack of fit to the data; that is, the error in the solution was not randomly distributed.

The results of the model analysis for birefringent data from Bryngdahl's second type of interferometer were that nonlinear regression methods gave the greatest precision.

On the basis of the studies of data analytical procedures for birefringent data from the two interferometers, the binary work done

during this study was done using Bryngdahl's first type of interfero-
meter and using a nonlinear curve-fitting computer program to fit
(2x) versus t measurements to Equation (5-1).

Uranyl Nitrate-Water System

The results of a study of the diffusion coefficient using bire-
fringence for the $UO_2(NO_3)_2$-H_2O system are presented below. These
diffusion coefficients are compared with diaphram cell data and
capillary cell data from the literature and are compared to ionic
diffusion theories.

Birefringent Diffusion Data

The diffusion coefficient of aqueous uranyl nitrate was measured
at eight concentrations between 0.00456 and 0.2459 molar. The bire-
fringent measurements were taken using Bryngdahl's first type of inter-
ferometer and were evaluated using a three-parameter, nonlinear,
curve-fitting technique. The mathematical model for this technique
was

$$y = 8B_1(t + B_2)\left(1 + \ln\left[\frac{t + B_2}{B_3 + B_2}\right]\right) \qquad (5-5)$$

where

$y = (2x)^2$ in cm

$t =$ time in sec

$B_1 =$ diffusion coefficient in $cm^2 sec^{-1}$

$B_2 = \Delta t$ time correction in sec

$B_3 =$ time of maximum y in sec

TABLE I

DIFFUSION COEFFICIENT DATA AND ERROR SUMMARY

Run Number	Average Concentration Molar	Diffusion Coefficient $\times 10^6$ cm^2 sec^{-1}	Average Diffusion Coefficient $\times 10^6$ cm^2 sec^{-1}	Standard Deviation $\times 10^6$ cm^2 sec^{-1}	Coefficient of Variance
4A		8.225			
4B	.2459	8.298	8.280	.048	.58
4C		8.316			
5A		8.636			
5B	.1032	8.517	8.557	.065	.76
5C		8.518			
6A		7.725			
6B	.0794	7.793	7.737	.051	.66
6C		7.693			
7A		7.888			
7B	.0489	7.966	7.888	.078	.99
7C		7.810			
8A		8.417			
8B	.0254	8.309	8.381	.062	.74
8C		8.416			
9B		8.781			
9C	.01003	8.766	8.782	.054	.61
9D		8.800			
10A		10.324			
10B	.00456	10.365	10.371	.038	.37
10C		10.423			
S11		14.767			
S12	.25	14.763	14.748	.029	.20
S13		14.715			
14B		7.940			
14C	.1617	7.878	7.878	.062	.79
14D		7.815			

A summary of the computer analysis of the birefringent data is contained in Appendix A. Table I contains the calculated value of D and an error summary.

The $UO_2(NO_3)_2$ data have an average coefficient of variance of 0.79. The coefficient of variance is defined as:

$$C.V. = \frac{\sigma \times 100}{\bar{D}} \qquad (5\text{-}6)$$

where

$$\sigma^2 = \frac{\sum_i (D_i - \bar{D})^2}{(i-1)} \qquad (5\text{-}7)$$

This error is consistent with the error expression derived and discussed in Appendix C.

The measurements from Runs 5 and 10 have been disregarded. Run 5 ($\bar{C}$ = .1023 M) was discarded because the solution heads were not equilibrated at the time the run was began. Run 10 is not usable because the concentration gradient was too small to give a sufficient number of (2x) measurements at sufficient times before maximum fringe pair separation. The error analysis, discussed in Appendix C, shows that (2x) measurements at late times during the diffusion run can result in a large systematic error.

Sample photographs of fringe patterns formed during diffusion Run 7A, $\bar{C}$ = 0.0487 M, are shown in Plate I. The photograph labeled t = 0 is a photograph of the initial interface. This photograph clearly shows that the initial interface is of finite thickness. Very thin fringes can be seen on either side of the initial interface.

PLATE I   Binary Diffusion Fringe Patterns
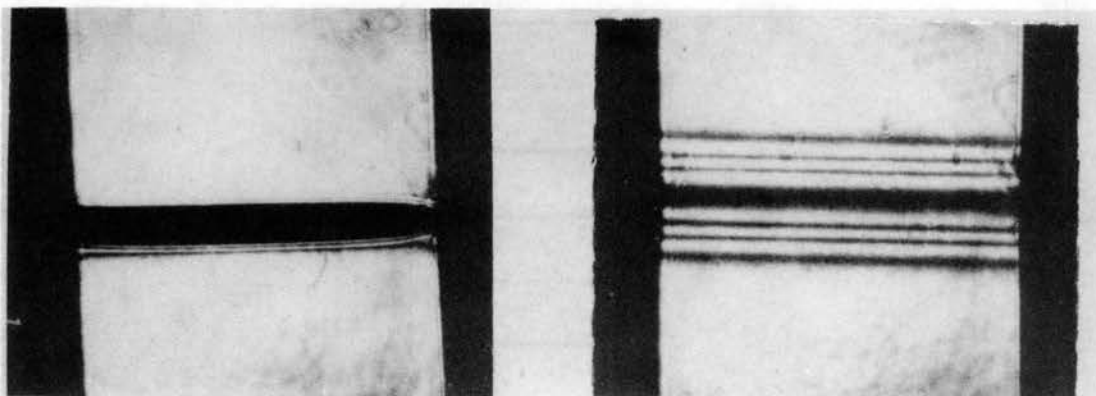
t = 0

t = 2 min
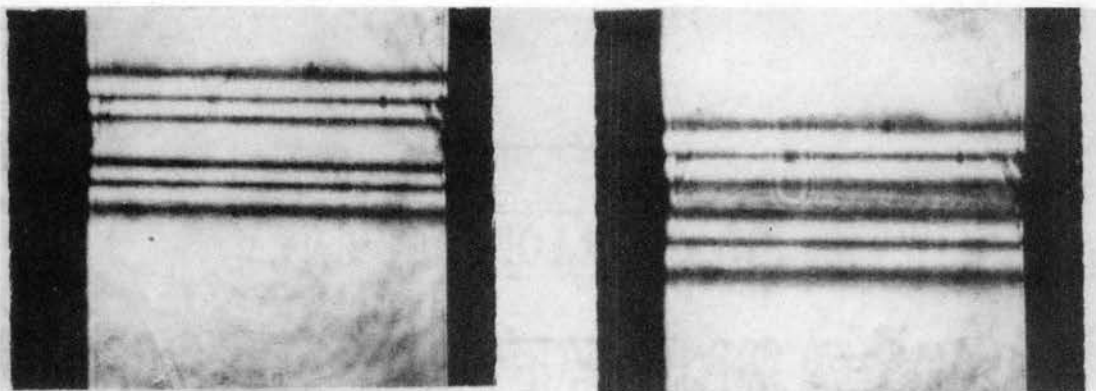
t = 3 min

t = 4 min
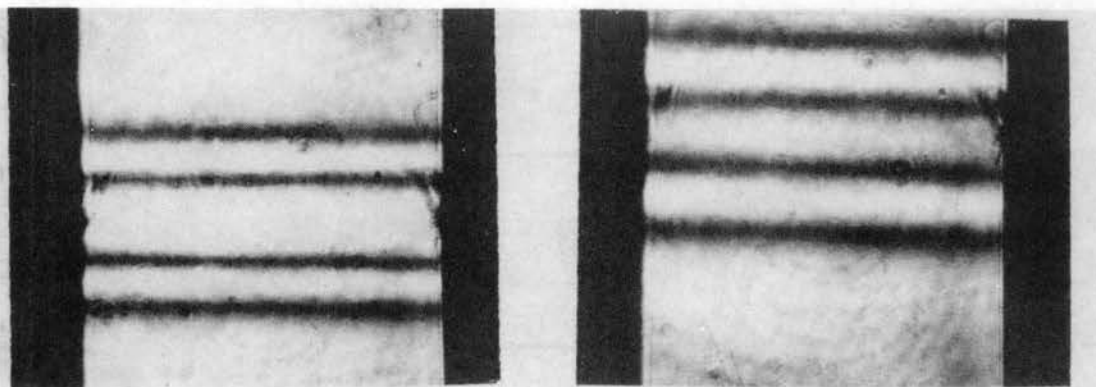
t = 7 min

t = 10 min

These fringes are indicative of concentration gradients in this region of the interface. The finite thickness of the interface and the presence of concentration gradients in the initial interface, support the need for a Δt time correction in diffusion coefficient determinations.

The initial interface photograph clearly shows that the interface is tapered on one side of the cell. This tapered effect is probably due either to varying slit width through the cell or to a particle of foreign material wedged in the slit opening, causing too rapid draw-off from one slit. The effect died away rapidly as can be seen in later photographs.

From the photographs presented in Plate I, the motion of the fringe pairs can be observed with time. Early in the diffusion time, the fringe pairs move away from the interface. At later times, the fringe pairs move back together and vanish at the initial position of the interface.

Comparison of the Data with Literature

The birefringent diffusion data are shown in Figure 3 along with integral diaphram cell data presented by Snyder (25) and capillary cell data as derived by Finley (10). The data obtained from the three different experimental methods are consistent at concentrations above 0.5 molar.

Snyder's diaphram cell data are consistently higher than the values of D from the birefringent method at concentrations above 0.5 molar. The two values of D measured by Snyder at concentrations below 0.02 molar are not consistent with optical diffusion observations.

Figure 3. Comparison of Diffusivities From Different Methods in the Uranyl Nitrate-Water System
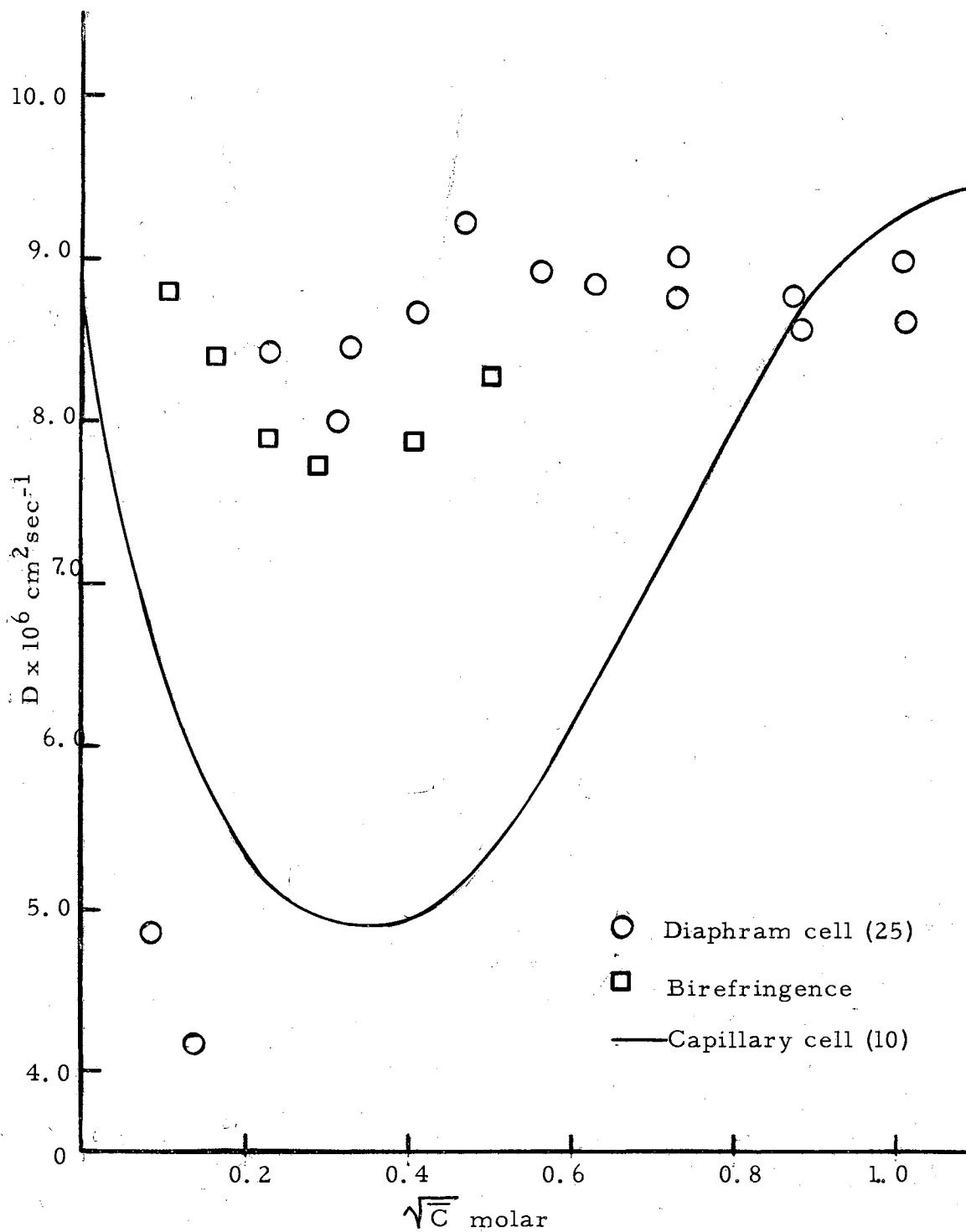
However, this inconsistency is not surprising, because the validity
of the diaphram cell method at such low concentrations has been
strongly questioned (26).

At concentrations lower than 0.5 molar, the optical diffusion
data are significantly higher than those predicted by Finley. The
birefringent diffusion data do not confirm the low values of D in the
0.1 M region as predicted by Finley.

Finley used a low value for the Nernst limiting value of the
diffusion coefficient, $D^O = 8.74 \times 10^{-6} cm^2 sec^{-1}$, to derive the dif-
ferential diffusion coefficient curve. New, more accurate transport
numbers have been published (14), and a new value of $D^O = 10.211 \times 10^{-6}$
$cm^2 sec^{-1}$ is calculated (see Appendix A for D^O calculation from these
new data). Had Finley used a higher value of D^O, his calculated
differential diffusion curve would not have predicted such low values
of D in dilute solutions.

In order to make a more meaningful comparison between the
capillary cell integral diffusion coefficients and optical differen-
tial coefficients, calculations modeling the diffusion in a capillary
cell were made. Table II summarizes these calculations.

Table II shows the initial and final average concentrations, $\overline{C}$,
observed by Finley. The calculated concentration averages are the
results of a numerical solution to the nonlinear, second order,
partial differential equation

$$\frac{\partial c}{\partial t} = \frac{\partial}{\partial t} \left[D(c) \frac{\partial c}{\partial t} \right] \qquad (5\text{-}8)$$

with 25 increments in distance down the capillary length and 434
increments in time. A derivation of the numerical expressions are

TABLE II

CAPILLARY CELL DIFFUSION COMPARISON

Diffusion Time (sec)	Capillary Length (cm)	$\bar{C}_{begin}$	$\bar{C}_{end}$	$\bar{C}_{calculated}$	
				Optical	Capillary
144,000	2.05590	.050	.022	.0195	.0237
144,000	2.05380	.250	.110	.1029	.1253

presented in Appendix E, and the computer program is contained in Appendix E.

As can be seen from Table II, calculations derived from optical data predict a lower value of $\bar{C}$ than that observed experimentally. Calculations using Finley's differential expression for D predict a higher value of $\bar{C}$ than that observed. These observations indicate that Finley's predicted values of D were consistently lower in this concentration range than the value of D from this birefringent study.

The function D(C) used in Equation (5-8) to evaluate Finley's predicted values was given by Finley (10). The function D(C) used in Equation (5-8) for this optical study was obtained from a nonlinear regression of the optical diffusion data. The functional form of D(C) was

$$D(C) = D_o + BC^P + EC^Q + FC^R + GC^S \qquad (5-9)$$

with

$P = 0.5$ $D_0 = 10.211 \times 10^{-6}$

$Q = 1.0$ $B = -16.61 \times 10^{-6}$

$R = 2.0$ $E = 28.561 \times 10^{-6}$

$S = 3.0$ $F = -9.13037 \times 10^{-6}$

C in molar concentration $G = -11.74 \times 10^{-6}$

D in $cm^2 sec^{-1}$

Figure 4 is a plot of Equation (5-9) with the optical data used for the regression. The regression has an average error of 0.67 per cent.

Comparison of optical data with data from the diaphram cell and capillary cell shows good agreement of the three methods at concentrations above 0.5 molar. However, the three methods disagree in the low concentration region. This disagreement between the methods is not surprising because the applicability of the diaphram cell and capillary cell methods has been questioned for dilute solutions in systems with rapid changes of diffusion coefficient with concentrations (21) (26).

Comparison of the Data to Ionic Diffusion Theories

One source of variation in the diffusion coefficient is attributed to nonideal behavior of the solution. The birefringent data from this work is corrected thermodynamically and compared to two ionic diffusion theories, the Nernst theory and the Stokes equation.

In order to correct the diffusion coefficient for the proper driving potential, the observed value of the diffusion coefficient must be corrected by using the thermodynamic correction factor,

Figure 4. Diffusion Coefficient of Uranyl Nitrate in Water
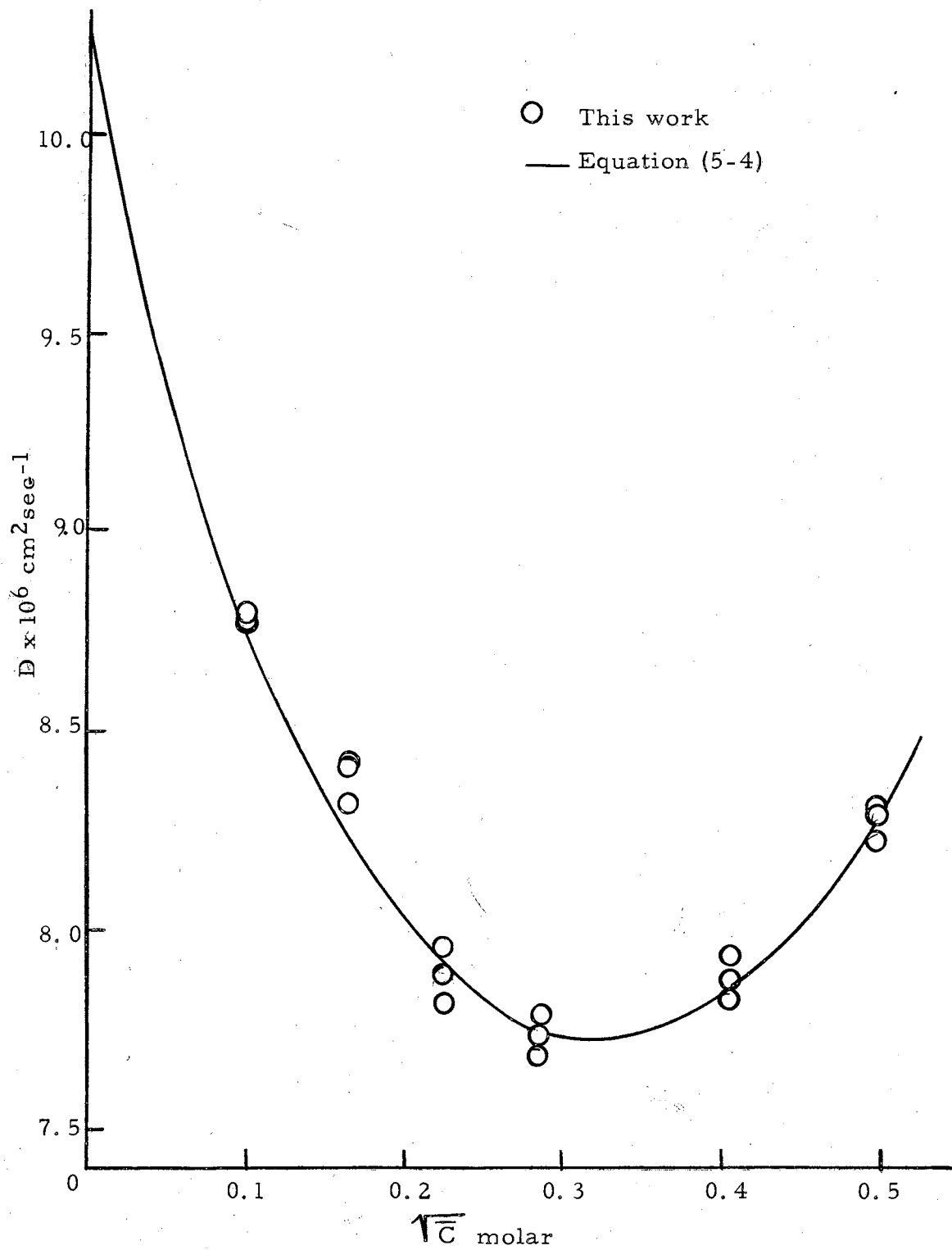
Equation (2-35). A plot of the thermodynamic correction factor versus concentration for the uranyl nitrate-water system is contained in Appendix A. The thermodynamic correction factor plot is similar to that of other divalent salts (21). The thermodynamic correction factor plot was calculated by means of a computer program presented in Appendix B. The program is based on the differentiation of the Harned and Owen (21) equation for the activity coefficient using data from Robinson and Stokes (21). This thermodynamic correction factor plot is similar to the numerical solution for the thermodynamic correction factor that Finley (10) presented.

Table III shows the birefringent data, the thermodynamic correction factor for each data point concentration, and the thermodynamically corrected diffusion coefficient.

A plot containing thermodynamic corrected diffusion data versus concentration from this work is presented with the integral capillary cell data from Finley and the diaphram cell data from Snyder in Figure 5.

Figure 5 shows the highly nonideal nature of the aqueous uranyl nitrate system. It is obvious from this figure that the thermodynamic correction alone is insufficient to describe the concentration dependence of diffusivities in the $UO_2(NO_3)_2$-H_2O system.

Ionic diffusion theories that are applicable to the $UO_2(NO_3)_2$-H_2O system are the expressions given by Stokes (25) and by Nernst (21). The Nernst equation, Equation (2-36), is applicable only as the concentration goes to zero. The Stokes equation, Equation (2-37), is applicable over the entire solution concentration range.

TABLE III

THERMODYNAMIC CORRECTION TO DIFFUSIVITIES

Run Number	Average Concentration (ML^{-1})	Thermodynamic Correction Factor	Diffusion Coefficient $cm^2\ sec^{-1}$	Thermodynamic Corrected Diffusion $cm^2\ sec^{-1}$
4	.2459	1.0453	8.280	7.721
5	.1032	.8920	8.557	9.593
6	.0794	.8744	7.737	8.848
7	.0489	.8591	7.888	9.182
8	.0254	.8600	8.381	9.745
9	.01003	.8817	8.782	9.960
10	.00456	.9060	10.371	11.447
14	.1617	.9464	7.878	8.324

The experimental data from this work are shown in Figure 6 with the Nernst limiting equation and the Stokes equation. Calculations for the Nernst limiting expression are in Appendix C. The Stokes equation was approximated by means of a computer program contained in Appendix B.

The data agree well with the Nernst limiting equation below 0.05 molar. The data qualitatively agree with the Stokes equation, but are consistently higher than the Stokes equation.

The thermodynamically corrected diffusivities have been compared to ionic diffusion theory for the $UO_2(NO_3)_2-H_2O$ system. The

Figure 5. Thermodynamic-Corrected Diffusion Coefficient
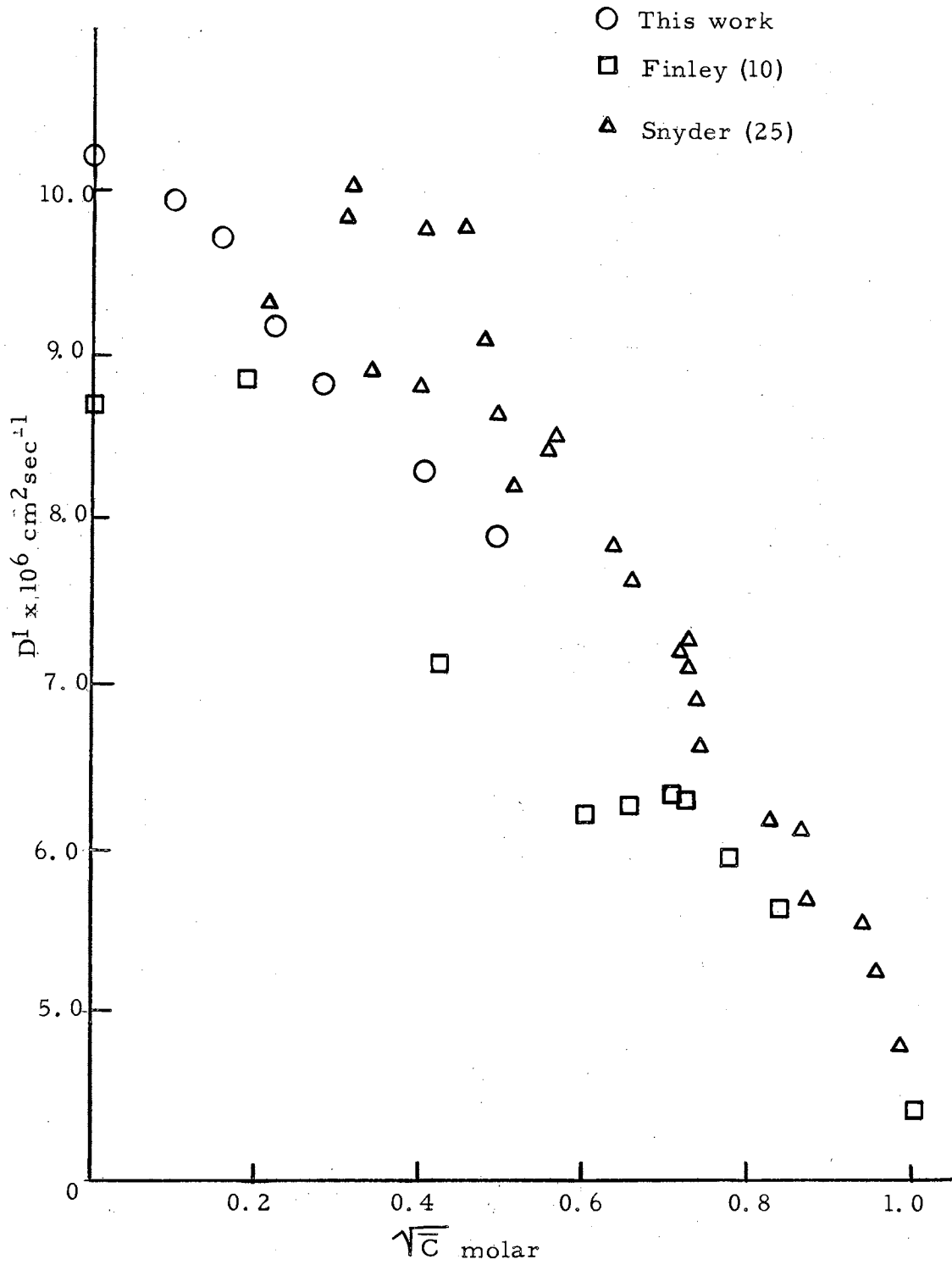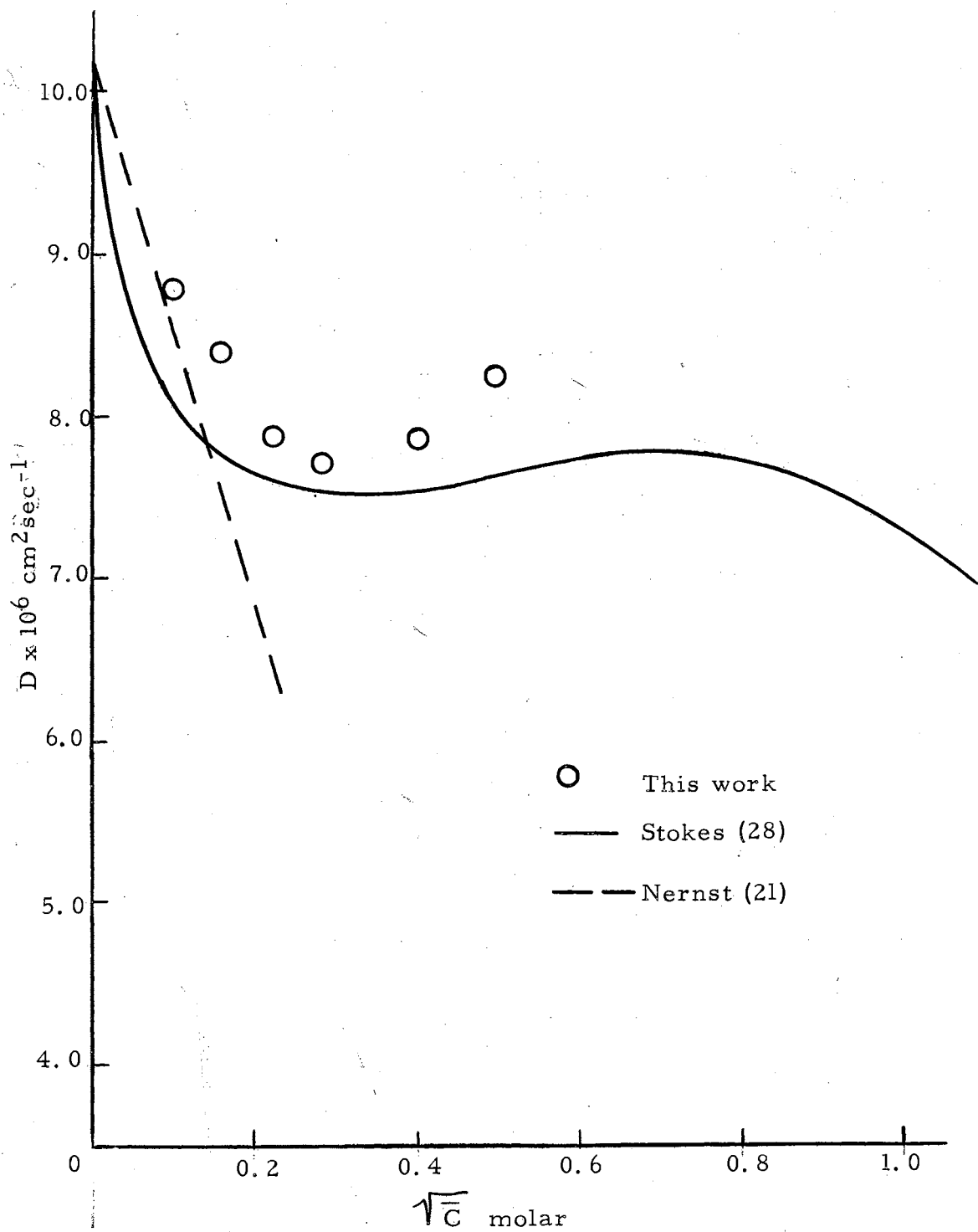of Uranyl Nitrate in Water

Figure 6. Comparison of Diffusion Data With Diffusion Theories in the Uranyl Nitrate System

diffusion data reflect highly nonideal behavior, but do agree qualitatively with ionic diffusion theory.

Uranyl Nitrate-Nitric Acid-Water System

One objective of this work was to qualitatively explore the use of birefringence methods in studying the uranyl nitrate-nitric acid-water system. Bryngdahl's second type of interferometer was chosen for this study because the interferometer produces a direct plot of the solution refractive index gradient (5).

Both cocurrent and countercurrent diffusion runs were made in this study. Cocurrent diffusion occurs when the driving forces for both components are in the same direction. When component driving forces are in opposite directions, the process is called counter-current diffusion. The solution to the diffusion equations, Equations (2-20) and (2-21), is similar for the cocurrent and countercurrent diffusion cases.

Several runs in the range of $\bar{C}_{UO_2(NO_3)_2} = 0.10$ and $\bar{C}_{HNO_3} = 0.50$ with varying ΔC were made. Plate II contains part of the results of these runs. The interference patterns for the cocurrent diffusion were all uni-peaked. In the cocurrent diffusion photographs of Plate II, the driving forces are $\Delta C_{UO_2(NO_3)_2} = 0.0053$ and $\Delta C_{HNO_3} = 0.027$.

Another ternary run was made by countercurrently diffusing a pure solution of 0.015 M uranyl nitrate into a pure solution of 0.09 M nitric acid. These concentrations were chosen because of minimum refractive index gradient and minimum density difference considerations required by our equipment. The results of this run are shown in Plate II. One will note that the refractive index gradient fringes

PLATE II   Ternary Diffusion Fringe Patterns

Countercurrent

Cocurrent
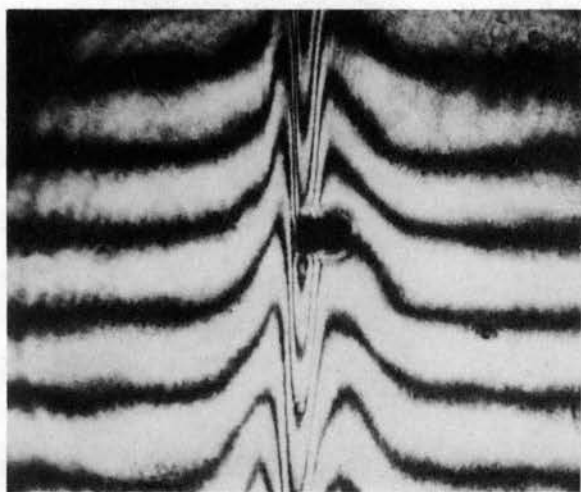
t = 1.0 min
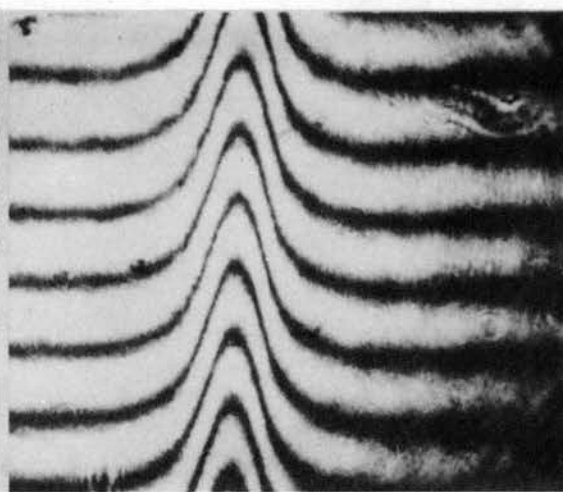
t = 1.0 min
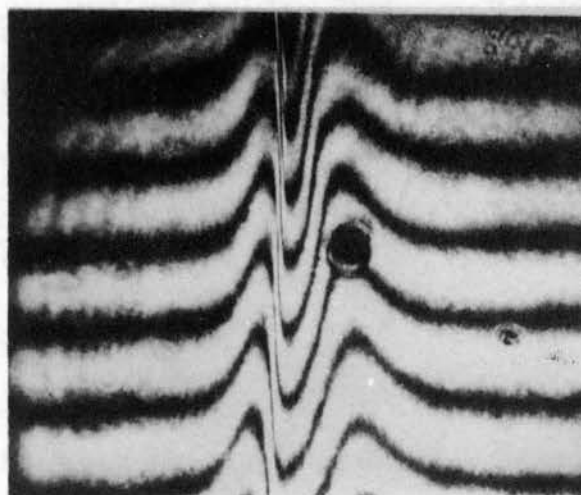
t = 5.0 min
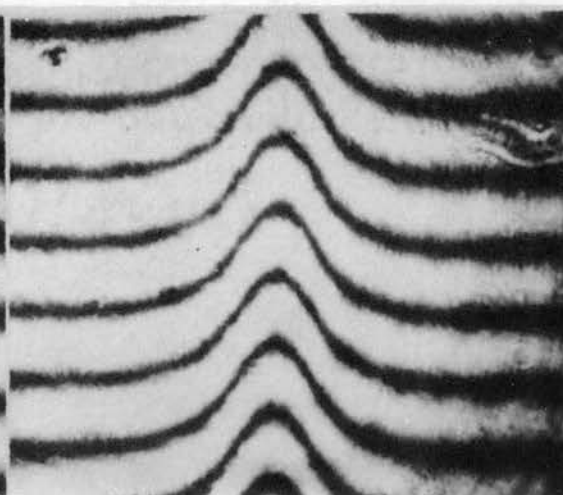
t = 2.5 min
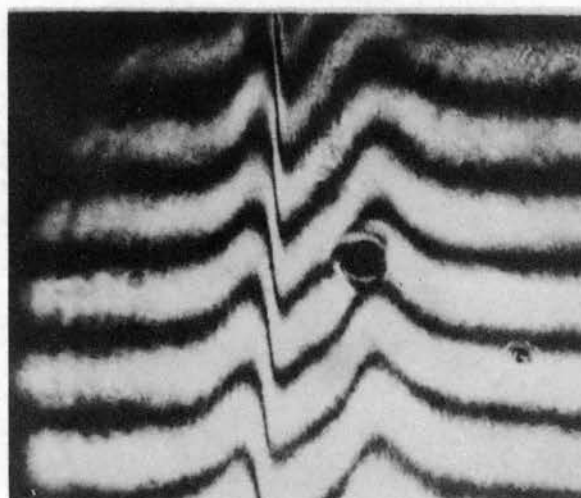
t = 8.0 min
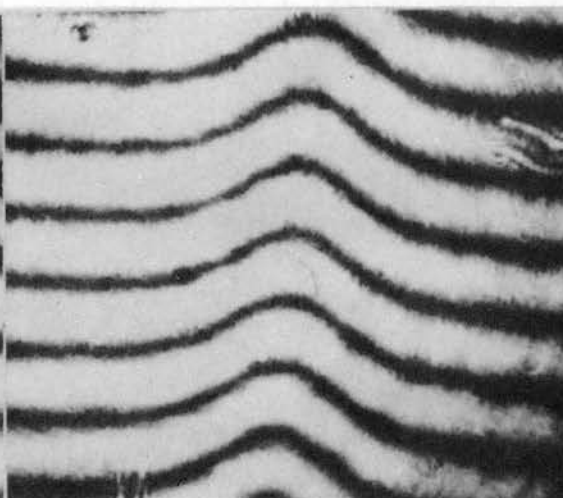
t = 6.0 min

are not only skewed but are also in a tri-peaked form.

Bryngdahl and Ljunggren (5) recorded the multi-peaked effect in a bottom layer diffusion experiment with 2.9 per cent sodium chloride and 0.1 per cent Dextran system. They qualitatively explained the phenomenon of two peaks by letting one peak represent one component and the second peak represent the second component.

In order to attempt to explain the phenomenon of three peaks, a computer program was developed to calculate refractive index gradient curves in a two-diffusing component system under the same boundary conditions as Equations (2-23), (2-24), (2-25), and (2-26). This was done by using a truncated Taylor expansion for the refractive index of a solution of two components (11),

$$n_{sol} = n_{slv} + R_1 C_1 + R_2 C_2 \qquad (5\text{-}10)$$

where R_1 and R_2 are differential refractive index increments.

Since Bryngdahl's second interferometer gives fringe patterns of the solution refractive index gradient curves, taking the derivative of Equation (5-10) with respect to the diffusion direction gives

$$\frac{\partial n_{sol}}{\partial x} = R_1 \frac{\partial C_1}{\partial x} + R_2 \frac{\partial C_2}{\partial x} \qquad (5\text{-}11)$$

where $\dfrac{\partial C_i}{\partial x}$ is determined from the exact solution. Thus

$$\frac{\partial c_i}{\partial x} = K_i^+ \sqrt{\frac{\sigma_+}{\pi t}} \exp\left(\frac{-\sigma_+ x^2}{4t}\right) + K_i^- \sqrt{\frac{\sigma_-}{\pi t}} \exp\left(\frac{-\sigma_- x^2}{4t}\right) \qquad (5\text{-}12)$$

Substituting Equation (5-12) with $i = 1, 2$ into Equation (5-11) gives an expression for the refractive index gradient value when D_{ij}'s, R_i's, ΔC_i's, distance (x), and time (t) are specified. Due

to the algebraic complexity involved here, this system was computer-
ized for convenience and the resulting program is in Appendix B.

Data on nitric acid were required. Density of the nitric acid-
water system were presented by Davis (7) and Perry (19). A cor-
relation of nitric acid-water system density was presented by Burger
(6). The International Critical Tables (18) has nitric acid diffusion
coefficient data. Luhdemann (15) has published refractive index
data, and Burger (6) has correlated refractive index data for nitric
acid.

The phenomena of negative cross term diffusion coefficients have
been reported previously (11) (20). Using this as a possible explana-
tion to the tri-peaked system observed, the program was run with the
following system assumed parameters.

$$D_{11} = 0.000050 \qquad C_{A1} = 0.015$$

$$D_{12} = -0.000015 \qquad C_{A2} = 0.0$$

$$D_{21} = 0.000001 \qquad C_{B1} = 0.0$$

$$D_{22} = 0.000004 \qquad C_{B2} = 0.09$$

$$R_1 = 0.008 \qquad R_2 = 0.035$$

The results of the refractive index gradient curve showed dis-
tinctly three peaks as was observed experimentally in the data pre-
sented in Plate II. The generated refractive index gradient curves
are given in Appendix B.

The program was also run using conditions similar to the pre-
viously mentioned cocurrent runs. And, as one would expect, a uni-
peaked refractive index gradient curve was the result.

This qualitative study of the diffusing uranyl nitrate-nitric

acid-water system showed the system exhibits multi-peaked refractive index gradients under countercurrent conditions. Cocurrent diffusion in the system gave unimodal refractive index gradient curves. Since this system exhibits unimodal refractive index gradient curves, a complete study of the ternary diffusivity of the system is feasible.

CHAPTER VI

CONCLUSIONS AND RECOMMENDATIONS

A study of mathematical models for evaluating birefringent data showed that nonlinear regression analytical methods gave the greatest precision.

The diffusion coefficient of aqueous uranyl nitrate was measured at eight concentrations between 0.00456 and 0.2459 molar. The birefringent measurements were taken using Bryngdahl's first type of interferometer and were evaluated using Equation (5-5) as the model for the nonlinear regression.

$$y = 8.0\, B_1(t + B_2) \left[1 + \ln\left(\frac{t + B_2}{B_3 + B_2}\right)\right] \qquad (5\text{-}5)$$

The diffusion coefficient of uranyl nitrate in dilute solutions has been expressed by assuming a polynomial relationship between the diffusion coefficient and the concentration. The relationship between the diffusion coefficient and the uranyl nitrate concentrations studied was determined as

$$D = 10.211 \times 10^{-6} - 16.61 \times 10^{-6}\, c^{.5}$$

$$+ 28.561 \times 10^{-6}\, c^{1.0} - 9.13037 \times 10^{-6}\, c^{2.0}$$

$$- 11.74 \times 10^{-6}\, c^{3.0} \qquad (6\text{-}1)$$

The diffusion coefficient measurements have been compared to measurements from both the capillary cell method and from the diaphram cell method. This comparison showed good agreement of the three methods at concentrations above 0.5 molar. However, the three methods disagree in the low concentration region. This disagreement between the methods reinforces arguments questioning the applicability of the diaphram cell and capillary cell methods for dilute solutions in systems with rapid changes of diffusion coefficient with concentrations.

The diffusion coefficient measurements have been compared to the Nernst and Stokes expressions, and have been corrected thermodynamically. The data are consistently higher than predicted by the Stokes equation. Correcting the data by using the thermodynamic correction factor did not adequately describe the effects that concentration has on the diffusion coefficient in the uranyl nitrate-water system.

The diffusion of the uranyl nitrate-nitric acid-water system has been observed. Sample runs have been presented. Under countercurrent conditions the system exhibits multi-peaked characteristics. Cocurrent diffusion in the system gave unimodal refractive index gradient curves. Experimental determination of the diffusion characteristics using cocurrent diffusion of the solutes is feasible.

Recommendations

The fringe measurement accuracy should be improved by measuring the outermost fringe pair.

Using experimental equipment which produces an optical density

plot, as was done by Bryngdahl, is recommended to improve fringe measurements.

Cylindrical constant head feed tanks should be installed in the present equipment.

Interface models should be developed to correct for the finite thickness of the initial interface. A good interface model would improve data analysis by giving a more random fit of the birefringent data. A good interface model would also allow the use of smaller concentration gradients in diffusion studies.

The uranyl nitrate-nitric acid-water system cocurrent diffusion should be studied using the birefringent interferometer. Models for diffusion measurements presented by Fugita are recommended for adoption to birefringent data.

SELECTED BIBLIOGRAPHY

1. Baldwin, R. L., R. J. Dunlop, and L. J. Gosting. J. Am. Chem. Soc., Vol. 77 (1955), 5235.

2. Bevilacqua, E. M., E. B. Bevilacqua, M. M. Bender, and J. W. Williams, Annals New York Academy of Sciences, Vol. 46 (1945), 309-21.

3. Bryngdahl, O. Acta Chemica Scandinavica, Vol. 11 (1957), 1017.

4. Bryngdahl, O. Acta Chemica Scandinavica, Vol. 12 (1958), 684.

5. Bryngdahl, O. and S. Ljunggren. J. Phys. Chem., Vol. 64 (1960), 1264.

6. Burger, L. L. and R. C. Forsman. U. S. Atomic Energy Commission Report. HW-20936 (1951).

7. Davis, W., Jr. and H. J. DeBruin. J. Inorg. Nucl. Chem., Vol. 26 (1964), 1069.

8. Edwards, O. W. J. Phys. Chem., Vol. 70 (1966), 217.

9. Erbar, J. H. Personal Communication.

10. Finley, J. B. Ph.D. Thesis. "Diffussion in Concentrated Uranyl Nitrate Systems." Oklahoma State University (1964).

11. Fugita, H. and L. J. Gosting. J. Am. Chem. Soc., Vol. 78 (1955), 1090.

12. Gouy, G. L. Paris Acad. Sci., Vol. 90 (1943), 307.

13. Graham, T. Phil. Magazine. (1861), 151, 183.

14. Hale, C. F. Ph.D. Thesis. "A Thermodynamic Investigation of Aqueous Uranyl Nitrate at 25 and 0° C." University of Colorado (1964).

15. Luhdemann, R. Z. Phisk. Chem., Vol. B29 (1935), 133.

16. Marquardt, D. W. J. Siam. (June, 1963), 431.

17. Mundy, R. J. U. S. Atomic Energy Commission Report. A-1052.

18. National Research Council, International Critical Tables of Numerical Data, McGraw-Hill, New York, 1933.

19. Perry, J. H., Editor. Chemical Engineering Handbook, 4th ed. McGraw-Hill, New York, 1963.

20. Philpot, J. and G. H. Cook. Research London, Vol. 1 (1948), 234.

21. Robinson, R. A. and R. H. Stokes. Electrolyte Solution, 2nd ed. Butterworths Scientific Publications, London, 1959.

22. Skinner, R. D. Ph.D. Thesis. "Initiation of Interfacial Turbulence in Liquid-Liquid Systems." Oklahoma State University (1967).

23. Slater, C. E. Personal Communication.

24. Slater, C. E. M.S. Thesis. "The Simultaneous Transfer of Uranyl Nitrate and Nitric Acid Across the Water-Tributyl Phosphate Interface." Oklahoma State University (1965).

25. Snyder, J. Personal Communication.

26. Tyrrell, H. J. V. Diffusion and Heat Flow in Liquids. Butterworths Scientific Publications, London, 1961.

27. Thomas, W. J. and E. McK. Nicholl. Applied Optics, Vol. 4 (1965), No. 7, 823.

28. Wishaw, B. F. and R. H. Stokes. J. Am. Chem. Soc., Vol. 76 (1954), 2065.

APPENDIX A

TABLE IV

REFRACTIVE INDEX OF AQUEOUS URANYL NITRATE

Concentration Moles/liter C	Scale Reading S	Refractive Index N
0.00000	0.4500	**1.33268**
0.01995	0.5750	1.33348
0.03995	0.6775	1.33414
0.05613	0.7500	1.33462
0.06054	0.7900	1.33477
0.08000	0.9150	1.33568
0.10106	1.0000	1.33622
0.21221	1.6200	1.34022
0.29921	2.0700	1.34310
0.39811	2.6150	1.34659
0.44899	2.8800	1.34828
0.50013	3.1650	1.35010
0.60381	3.7000	1.35350
0.70169	4.2200	1.35680
0.90474	5.3200	1.36373
1.00207	5.8700	1.36717
1.13623	6.5650	1.37150
1.29968	7.3900	1.37661
1.49998	8.5000	1.38345
1.61202	9.1150	1.38720
1.81182	10.2150	1.39388
2.00678	11.1750	1.39966

The refractometer scale reading was calibrated for concentration calculations. Results of a linear least squares fit of the model $S = mC + b$ are:

$$m = 5.356511$$

$$b = 0.469427$$

$$\sigma^2 = 0.019740$$

TABLE V

SPECTROPHOTOMETER CALIBRATION

Total Micro Moles in Samples	Absorption	
10.1230	1.68	1.68
9.1007	1.50	1.50
8.0984	1.33	1.32
7.0861	1.18	1.18
6.0738	1.00	1.01
5.0615	0.811	0.815
4.0492	0.668	0.681
3.0369	0.541	0.551
2.0246	0.341	0.353

Results of a linear least squares fit for the model $A = mC + b$ are:

$$m = 161.8$$

$$b = 0.021$$

where:

A = Absorption reading

C = Concentration (molar)

TABLE VI

COMPUTER ANALYSIS OF EXPERIMENTAL DATA

Run Number	$D \times 10^6$ (cm^2/sec)	$\Delta T(sec)$	$t_i(sec)$	Average Error (%)	$\sum\left[\Delta(2x)^2\right]$ $(\times 10^{12}\ cm^2)$
4A	8.225	31.2	232.7	1.59	1.908
4B	8.298	32.6	233.4	1.03	.604
4C	8.316	35.4	236.5	1.09	.486
5A	8.636	21.3	213.4	2.01	.804
5B	8.517	7.0	260.1	1.25	1.070
5C	8.518	8.5	260.4	1.89	3.282
6A	7.725	42.4	289.5	1.20	1.214
6B	7.793	39.7	291.8	1.11	1.827
6C	7.693	39.4	295.1	0.96	1.215
7A	7.888	46.2	269.3	1.55	1.629
7B	7.966	44.2	268.5	1.28	1.415
7C	7.810	47.8	271.2	1.56	1.813
8A	8.417	36.3	279.3	.95	.788
8B	8.309	35.9	284.1	.60	.325
8C	8.416	36.5	279.1	1.30	1.544
9B	8.781	40.6	258.0	1.88	3.929
9C	8.766	40.1	258.4	1.81	3.923
9D	8.800	36.4	261.2	1.14	.994
10A	10.324	29.3	41.7	1.97	.096
10B	10.365	27.2	42.0	2.26	.296
10C	10.423	29.3	40.7	3.89	.387
S11	14.767	19.4	298.7	.73	1.615
S12	14.763	20.2	296.4	.57	1.108
S13	14.715	22.0	297.4	.53	.812
14B	7.940	54.1	283.1	1.03	1.038
14C	7.878	56.2	284.5	1.41	2.072
14D	7.815	55.5	284.5	1.33	1.570

Figure 7. Thermodynamic Correction Factor For Aqueous
Uranyl Nitrate
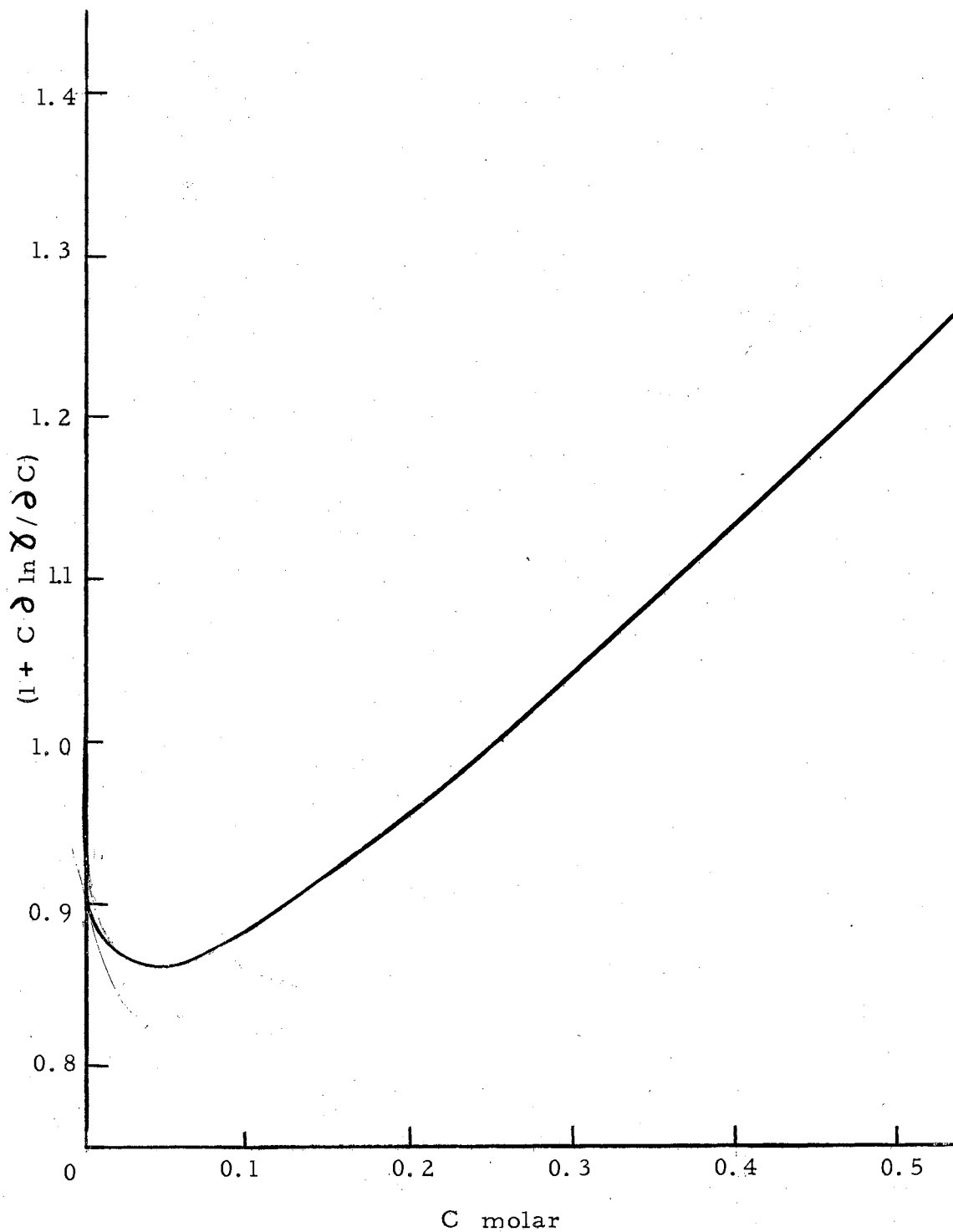
APPENDIX B

```
$ID         A-0001 METZ                        2507-40074
$JOB               METZ                        2507-40074
$IBJOB NAMEPR  MAP
$IBFTC
   99 FORMAT (7F14.7)
   98 FORMAT (50H    D11           D12          D21         D22
   97 FORMAT (50H  CA1      CA2      CB1       CB2      DC1      DC2
   96 FORMAT(50H  DC1DX      DC2DX      DNDX       X      T
      DIMENSION AX(1000), AY(1000), AZ(1000)
      SUBSCRIPT 1 =ACID
      SUBSCRIPT 2 = UO2(NO3)2
      PI=22.0/7.0
      R1=0.008
      R2=0.035
      D11=0.0000115
      D12=-.00001
      D21=0.000005
      D22=0.000008
      CA1=0.015
      CA2=0.0
      CB1=0.0
      CB2=0.09
      CBAR1=(CA1+CB1)/2.0
      CBAR2=(CA2+CB2)/2.0
      DC1=(CB1-CA1)
      DC2=(CB2-CA2)
      WRITE (6,98)
      WRITE (6,99) D11, D12, D21, D22
      WRITE (6,97)
      WRITE (6,99)CA1, CA2, CB1, CB2, DC1, DC2
      DENOM=4.0*((D22-D11)**2  +4.0*D12*D21)**0.5
      DUMY=((D22-D11)**2  +4.0*D12*D21)**0.5
      AK1P=((D22-D11+DUMY)*DC1-2.0*D12*DC2)/DENOM
      AK1M=((D22-D11-DUMY)*DC1-2.0*D12*DC2)/DENOM*(-1.0)
      AK2P=((D11-D22+DUMY)*DC2-2.0*D21*DG1)/DENOM
      AK2M=((D11-D22-DUMY)*DC2-2.0*D21*DC1)/DENOM*(-1.0)
      AGMP=(D22+D11+((D22-D11)**2  +4.0*D12*D21)**0.5)/
     1(2.0*(D11*D22-D12*D21))
      AGMM=(D22+D11-((D22-D11)**2  +4.0*D12*D21)**0.5)/
     1(2.0*(D11*D22-D12*D21))
      WRITE (6,99) DENOM, DUMY, AGMP, AGMM
      BGMP=ABS(AGMP)
      BGMM=ABS(AGMM)
      T=30.0
      NPLOT=0
      NPTS=0
   78 DX=0.01
      WRITE (6,96)
      X=-0.40000000
      MM=81
      DO 79 K=1,MM
      DC1DX=AK1P*(BGMP)**0.5*EXP(-AGMP*X**2  /(4.0*T    ))/((T*PI)**.5)
      DUMY=+AK1M*(BGMM)**0.5*EXP(-AGMM*X**2  /(4.0*T    ))/((T*PI)**.5)
      DC1DX=DC1DX+DUMY
      DC2DX=AK2P*(BGMP)**0.5*EXP(-AGMP*X**2  /(4.0*T    ))/((T*PI)**.5)
      DUMY=+AK2M*(BGMM)**0.5*EXP(-AGMM*X**2  /(4.0*T    ))/((T*PI)**.5)
      DC2DX=DC2DX+DUMY
      DNDX=R1*DC1DX+R2*DC2DX
      YP=X*(BGMP)**0.5/(2.0*T)
      YM=X*(BGMM)**0.5/(2.0*T)
      AERFP=ERF(YP)
      AERFM=ERF(YM)
      C1=CBAR1+AK1P*AERFP   +AK1M*AERFM
      C2=CBAR2+AK2P*AERFP   +AK2M*AERFM
      WRITE (6,99) DC1DX, DC2DX, DNDX, X, T ,C1, C2
      I=K+NPTS
      AY(I)=DNDX
      AX(I)=X
   79 X=X+DX
      NPTS=NPTS+MM
      NPLOT=NPLOT+1
      T=T+60.0
      DUMY=T-300.
      IF (DUMY) 78,77,77
   77 CONTINUE
      CALL PLOT(AX,0,AY,0,AZ,0,NPTS,NPLOT,0,3,2,0,2)
      STOP
      END
$ENTRY
   DN/DX VERSES  X  FOR DIFFERENT TIMES1 2 3 ...
      DN/DX                              .*',0=         X      X       X
$IBSYS
```

TABLE VII

SAMPLE COMPUTER OUTPUT FOR TERNARY DIFFUSION SOLUTION MODEL

Assumed input data were:

$$D_{11} = 0.000050 \ cm^2 sec^{-1} \qquad R_1 = 0.008$$

$$D_{12} = -0.000015 \ cm^2 sec^{-1} \qquad R_2 = 0.035$$

$$D_{21} = 0.000001 \ cm^2 sec^{-1} \qquad \triangle c_2 = 0.015 \ M/L$$

$$D_{22} = 0.000004 \ cm^2 sec^{-1} \qquad \triangle c_1 = -0.090 \ M/L$$

x (cm)	$\partial n/\partial x$ t = 16 sec	$\partial n/\partial x$ t = 31 sec	$\partial n/\partial x$ t = 61 sec
-0.1600000	-0.0000013	-0.0000443	-0.0002439
-0.1500000	-0.0000033	-0.0000733	-0.0003149
-0.1400000	-0.0000083	-0.0001173	-0.0004001
-0.1300000	-0.0000193	-0.0001819	-0.0004999
-0.1200000	-0.0000424	-0.0002730	-0.0006144
-0.1100000	-0.0000875	-0.0003965	-0.0007422
-0.1000000	-0.0001694	-0.0005576	-0.0008788
-0.0900000	-0.0003080	-0.0007591	-0.0010056
-0.0800000	-0.0005257	-0.0009999	-0.0010502
-0.0700000	-0.0008427	-0.0012673	-0.0007714
-0.0599999	-0.0012682	-0.0014744	0.0004681
-0.0499999	-0.0017789	-0.0010937	0.0039306
-0.0399999	-0.0020197	0.0020485	0.0112953
-0.0299999	0.0015382	0.0131409	0.0234711
-0.0199999	0.0239104	0.0369107	0.0387367
-0.0099999	0.0770531	0.0664024	0.0520537
0.0000001	0.1120873	0.0805259	0.0574052
0.0100001	0.0770525	0.0664022	0.0520536
0.0200001	0.0239100	0.0369104	0.0387366
0.0300001	0.0015381	0.0131407	0.0234709
0.0400001	-0.0020197	0.0020484	0.0112952
0.0500001	-0.0017789	-0.0010937	0.0039306
0.0600001	-0.0012682	-0.0014744	0.0004681
0.0700000	-0.0008427	-0.0012673	-0.0007714
0.0800000	-0.0005257	-0.0009999	-0.0010502
0.0900000	-0.0003080	-0.0007591	-0.0010056
0.1000000	-0.0001694	-0.0005576	-0.0008788
0.1100000	-0.0000875	-0.0003965	-0.0007422
0.1200000	-0.0000424	-0.0002730	-0.0006144
0.1300000	-0.0000193	-0.0001819	-0.0004999
0.1400000	-0.0000083	-0.0001173	-0.0004001
0.1500000	-0.0000033	-0.0000733	-0.0003149
0.1600000	-0.0000013	-0.0000443	-0.0002439

Computer Program For the Thermodynamic Correction

Factor and For the Stokes Equation

```
$IBSYS
$ENDWATFOR
$IBSYS
$WATFOR
$JOB 2507-40074,KP=26   W P METZ
C       CL=MOLAL CONC
C       CR = MOLAR CONC
C       GRP1 = THERMO CORRECTION FACTOR
C       ALPHA = DEGREE OF DISSOCIATION
        DIMENSION CL(20),CR(20),DEL1(20),DEL2(20),DENOMA(20),A(20),B(20)
        DIMENSION GRP1(20),GRP2(20),GRP3(20),DENOMC(20),ALPHA(20),GRP4(20)
        DIMENSION VIS(20),GRP5(20),D(20)
    10 FORMAT (F6.3,3E12.4)
    20 FORMAT (2F10.6,2E12.4)
    30 FORMAT (2F10.6,F10.4,F10.4,E12.4)
        READ (5,10) WH,DH2O,DO,D12
        N=25
        DO 100 I=1,N
        READ(5,20) CL(I),CR(I),DEL1(I),DEL2(I)
        DENOMA(I)= 1.0 + 2.66*(CL(I)**.5)
        A(I) = 1.0+.6909*CL(I)+(5.32*CL(I))/(DENOMA(I)**2)
        B(I) =(2.0*(CL(I)**.5))/DENOMA(I)
        GRP1(I) = A(I) - B(I)
        GRP2(I) = 1.0 - .01*CL(I)*WH
        GRP3(I) = 1.0 + .018*CL(I)*(((2.0*DH2O)/DO)-WH)
        DENOMC(I) = 1.0 +2.86*(CR(I)**.5)
        ALPHA(I) = 1.0-((1.34*(CR(I)**.5))/DENOMC(I))-0.22*CR(I)
        GRP4(I) = ALPHA(I)*(DO+DEL1(I)+DEL2(I))+2.0*(1.0-ALPHA(I))*D12
        VIS(I) = 9.069 + (3.411*CR(I)) + (3.504*(CR(I)**2))
        GRP5(I) =   0.8903/VIS(I)
        D(I) = GRP1(I)*GRP2(I)*GRP3(I)*GRP4(I)*GRP5(I)
   100 WRITE(6,30) CL(I),CR(I),GRP1(I),ALPHA(I),D(I)
        END
$ENTRY
   7.0       2.5700E-5  10.2200E-6    5.2000E-6
      .00         .00        .0000E-6     .0000E-6
      .05         .04963     -1.6900E-6   .3640E-6
      .1          .09923     -1.8200E-6   .3670E-6
      .2          .19699     -2.1300E-6   .3650E-6
      .3          .29328     -2.2400E-6   .3570E-6
      .4          .38813     -2.3400E-6   .3420E-6
      .5          .48159     -2.3800E-6   .3340E-6
      .6          .57368     -2.4800E-6   .3220E-6
      .7          .66449     -2.5000E-6   .3120E-6
      .8          .75395     -2.5500E-6   .2030E-6
      .9          .84213     -2.5700E-6   .2970E-6
     1.0          .92905     -2.6000E-6   .2870E-6
     1.2         1.09929     -2.6300E-6   .2770E-6
     1.4         1.26479     -2.6800E-6   .2650E-6
     1.6         1.4287      -2.7300E-6   .2570E-6
     1.8         1.58256     -2.7400E-6   .2500E-6
     2.0         1.73509     -2.7500E-6   .2420E-6
  .3261
  .1929
  .1151
  .0862
  .0514
  .0261
  .01013
  .00458
$IBSYS
```

APPENDIX C

APPENDIX C

DATA ANALYSIS METHODS

Linearization of the Two-Point Method

Equation (2-13) is the two-point solution to Equation (2-2) using boundary conditions (2-4) and (2-5).

$$D = \frac{x_2^2 - x_1^2}{4t \ln \dfrac{H_1}{H_2}} \tag{2-13}$$

Rearranging Equation (2-13) in a linear form gives

$$\ln \frac{H_1}{H_2} = \left(\frac{1}{4Dt}\right)\left(x_2^2 - x_1^2\right) \tag{C-1}$$

where $\dfrac{1}{4Dt}$ is the slope of the regression line, and the intercept is zero.

Linearization of the Four-Point Method

Equation (2-15) is the four-point solution to Equation (2-2) using boundary conditions (2-4) and (2-5).

$$D = \frac{(x_2'^2 - x_1'^2) - B(x_4'^2 - x_3'^2)}{4t(\Theta_{12} - \Theta_{34} B)} \tag{2-15}$$

Rearranging this equation in a linear form gives

$$(\Theta_{12} - \Theta_{34} \, B) = \frac{1}{4Dt} \left[(x_2^{'2} - x_1^{'2}) - B \, (x_4^{'2} - x_3^{'2}) \right] \qquad (C-2)$$

where $\frac{1}{4Dt}$ is the slope of the regression line and the intercept is zero.

Area-Moment Method

The solution to Fick's Second Law is of Gaussian form (2). That is, the solution can be represented by

$$H = \frac{N \, \omega}{2 \, \sigma \sqrt{\pi}} \exp \left[\frac{-(x - B)^2 \omega^2}{\sigma^2} \right] \qquad (C-3)$$

where ω is an arbitrary constant and

$$\sigma^2 = \mu_2 - \mu_1^2 \qquad (C-4)$$

$$\mu_2 = \frac{\sum H_i s_i^2}{\sum H_i} \qquad (C-5)$$

$$\mu_1 = \frac{\sum H_i s_i}{\sum H_i} \qquad (C-6)$$

$$N = \sum H_i \qquad (C-7)$$

Applying Equation (2-7) into Equation (C-3) and solving for D gives

$$D = \left[\frac{\sum s_i^2 H_i}{\sum H_i} - \left(\frac{\sum s_i H_i}{\sum H_i} \right)^2 \right] \frac{\omega^2}{2t} \qquad (C-8)$$

where H_i is the height of the refractive index gradient curve at the distance $s_i \, \omega$ from an approximated centroid, s_i is an integer, t is

time, and ω is a constant.

A standard solution of sodium chloride at $\bar{C} = 0.25$ M was used to obtain birefringent data to evaluate Equation (C-8). The literature value of the diffusion coefficient for this standard is 1.475×10^{-5} cm^2/sec. The results of this data evaluation are

Time (sec)	$Dx10^5, cm^2/sec$
150	2.112
150	2.150
120	2.204
120	2.252
90	2.564
90	2.548

These diffusion coefficients are not time corrected. Time correction of data, using Equation (2-14), gives an average value of $D^t = 1.496 \times 10^{-5} cm^2/sec$ with an average error of one per cent.

Nonlinear Evaluation

The results of a nonlinear evaluation of the model Equation (5-9) were

Time	$\dfrac{1}{2Dt}$
90	224.181
90	225.041
120	184.242
120	182.200
150	150.070
150	148.520

These results show an error of about one per cent in the reproducibility of D.

The results of evaluation of the model, Equation (5-10), were

t	$\dfrac{1}{4Dt}$	B_4
90	224,011	0.155
90	225.026	0.2837
120	184.124	0.2404
120	181,694	0.1967
150	150.018	0.1508
150	148.471	0.1249

where time is in seconds, D is in cm^2/sec, and B_4 is in sec^{-1}. The reproducibility in the diffusion coefficient is approximately one per cent. The skewed parameter, B_4, is indicative of the error in the base line approximation for the refractive index gradient curve.

Calculation of Nernst Limiting Values

Harned and Owen (21) discuss the method of obtaining a limiting equation for the diffusion coefficients of a single salt. From the Onsager-Fuoss theory for dilute solutions, it is shown that the limiting equation is

$$D = D_o - \mathscr{S}_{(D)} \sqrt{c} \qquad \text{(C-10)}$$

where

$$\mathscr{S}_{(D)} = \frac{1.3273 \times 10^{-3} \ (\sum v_i z_i^2)^{3/2}}{\mathscr{E}^{3/2} T^{1/2} \ \ v_1 |z_1|} \left[\frac{\lambda_1^o \ \lambda_2^o}{\Lambda^o} \right]$$

$$+ \frac{2.604 \times 10^{-8} \ (\sum v_i z_i^2)^{1/2}}{\eta_o \ \mathscr{E}^{1/2} T^{-1/2} \ |z_1 z_2|} \left[\frac{|z_2| \ \lambda_1^o - |z_1| \lambda_2^o}{\Lambda^o} \right]^2 \qquad \text{(C-11)}$$

and

$$D_o = 8.936 \times 10^{-10} \ T \ \frac{(v_1 + v_2)}{v_1 |z_1|} \ \frac{\lambda_1^o \ \lambda_2^o}{\Lambda^o} \qquad \text{(C-12)}$$

The quantities in the equation are:

v_i = number of cations, anions produced by dissociation of one molecule of electrolyte.

z_i = valences of ions indicated (carry sign of charge).

λ_i^o = limiting equivalent conductances of ions indicated at infinite dilution.

Λ^o = limiting equivalent conductance of electrolyte at infinite dilution.

η_o = viscosity of solvent.

$\mathscr{E}$ = dielectric constant of solution.

Designating the nitrate ion as one and the uranyl ion as two, the values for uranyl nitrate are found to be:

$V_1 = 1.0$

$V_2 = 2.0$

$Z_1 = 2.0$

$\lambda_1^o = 39.9 \ (10)$

$\lambda_2^o = 71.44 \ (14)$

$\Lambda^o = \lambda_1^o + \lambda_2^o = 39.9 + 71.44 = 111.34$

$T = 25^oC = 298^oK$

$\mathscr{E} = 80 - 0.4(t-20^o) = 80 - 0.4(25-20) = 80 - 2.0 = 78.0$

$\eta_o = .008903$ poise

$D_o = 8.936 \times 10^{-10}(298) \ \dfrac{3}{2.0} \ \dfrac{(39.9)(71.44)}{111.34}$

$D_o = 10.221 \times 10^{-6} cm^2 sec^{-1}$

thus:

$$\mathscr{E}_{(D)} = \frac{1.3273 \times 10^{-3}}{(78)^{3/2}(298)^{1/2}} \ \frac{\left[(1.0)(4.0)+(2.0)(1.0)\right]^{3/2}}{(1.0)(2.0)} \left[\frac{(39.9)(71.44)}{111.34}\right]$$

$$+ \ \frac{2.604 \times 10^{-8}}{(.8903)(78)^{1/2}(298)^{-1/2}} \ \frac{(6)^{1/2}}{2} \ \frac{(1)(39.9) - (2)(71.44)}{111.34}^2$$

$$= 8.2024 \times 10^{-7} \ (20.180) + 7.002 \times 10^{-8} \ (0.8555)$$

$$\mathscr{E}_{(D)} = 16.612 \times 10^{-6}$$

and finally the limiting expression for a dilute solution of uranyl nitrate is

$$D = 10.221 \times 10^{-6} - 16.612 \times 10^{-6} \sqrt{c} \tag{C-13}$$

The calculated coefficients will vary somewhat, depending on the data source of the limiting conductance values chosen for the ions.

Derivation of Systematic Error Expression

The estimated error in a dependent variable y due to the error observed in independent noninteracting variables is:

$$S_y^2 = \sum_n S_{x_i}^2 \left(\frac{\partial y}{\partial x_i} \right)^2 \tag{C-14}$$

where $y = y(x_i)$; S_i = standard deviation of i; and $x_j \neq f(x_i)$, $j \neq i$. Thus, if D is a function of (2x) and t only,

$$S_D^2 = S_{(2x)}^2 \left(\frac{\partial D}{\partial (2x)} \right)^2 + S_t^2 \left(\frac{\partial D}{\partial t} \right)^2 \tag{C-15}$$

using the identity $\ln e = 1.0$ and rearranging Equation (2-9) gives

$$D = \frac{(2x)^2}{8t \ln\left(\frac{et_i}{t}\right)} \tag{C-16}$$

Differentiating Equation (C-16) with respect to (2x)

$$\frac{\partial D}{\partial (2x)} = \frac{2(2x)}{8t \ln\left(\frac{et_i}{t}\right)} = \frac{2D}{(2x)} \tag{C-17}$$

Differentiating Equation (C-16) with respect to t

$$\frac{\partial D}{\partial t} = \frac{\partial}{\partial t} \left[\frac{(2x)^2}{8} (t)^{-1} \left(\ln^{-1} \frac{et_i}{t} \right) \right]$$

$$= \frac{(2x)^2}{8} \left[\frac{-1}{t^2 \ln \frac{et_i}{t}} + \frac{1}{t^2 \ln^2 \frac{et_i}{t}} \right]$$

and simplifying

$$= \frac{(2x)^2}{8t^2 \ln \frac{et_i}{t}} \left[-1 + \frac{1}{\ln \frac{et_i}{t}} \right]$$

$$\frac{\partial D}{\partial t} = \frac{D}{t} \left[\frac{1}{\ln \frac{et_i}{t}} - 1 \right] \tag{C-18}$$

Substituting (C-17) and (C-18) into (C-15) and rearranging:

$$S_D^2 = S_{(2x)}^2 \frac{4D^2}{(2x)^2} + S_t^2 \frac{D^2}{t^2} \left[\frac{1}{\ln \frac{et_i}{t}} - 1 \right]^2$$

$$\left(\frac{S_D}{D} \right)^2 = \left(\frac{2S_{(2x)}}{(2x)} \right)^2 + \left(\frac{S_t}{t} \right)^2 \left[\frac{1}{\ln \frac{et_i}{t}} - 1 \right]^2 \tag{C-19}$$

Let $\Phi = \dfrac{1}{\ln \frac{et_i}{t}} - 1 = \dfrac{\ln \frac{t}{t_i}}{\ln \frac{et_i}{t}}$ $\tag{C-20}$

then

$$\left(\frac{S_D}{D} \right)^2 = \left(\frac{2S_{(2x)}}{(2x)} \right)^2 + \left(\frac{S_t}{t} \right)^2 \Phi^2 \tag{C-21}$$

There are two major conclusions to be drawn from Equation (C-21): (a) that an error in (2x) measurement gives twice that error in the diffusion calculation, and (b) the factor, Φ , goes to infinity as time approaches et_i. This second conclusion emphasizes the fact that (2x) measurements at longer times during the run are not only poor due to fringe fuzziness, but they also contain a potentially large error due to time error, S_t, multiplication. Thomas and Nicholl (27) noted that their best measurements were made at the peak of the $(2x)^2$ versus time curve and that the small (2x) measurements at very short and very long times were not used.

Sample Error Calculation

The variance in the diffusion coefficient can be approximated using Equation (C-21). Fringe measurement reproducibility was in the range of 0.3 per cent. Time measurement error is approximated by human reaction time, about 0.2 sec. Using these errors for a diffusion coefficient calculation at $t = t_i = 300$ sec gives

$$\frac{S_D^2}{D} = (2 \times 0.3)^2 + \left(\frac{0.2}{300}\right)^2 \Phi^2$$

At $t = t_i$, the factor, $\Phi = 0$ and

$$\frac{S_D}{D} = 0.6\%$$

The average deviation in the diffusion coefficient was found to be 0.76.

The above calculations show that the error contribution due to

time is negligibly small compared to the error contribution due to fringe measurement. However, as time of fringe measurement goes to et_i (the time at which the fringe pair converge together), the factor, ϕ , goes to infinity and the expected error in the calculation of D also goes to infinity.

APPENDIX D

APPENDIX D

Analysis of Aqueous Nitric Acid in the

Presence of Uranyl Nitrate

Conductiometric titration is a familiar analytical method in
electro chemistry. It is based on the principle that the inverse
of the electrical resistance of a solution varies linearly with the
concentration of electrolyte in the dilute range - generally less
than 0.05 equivalents per liter.

In a strong acid-strong base neutralization titration, a V-
shaped conductivity curve is found. For a strong acid-weak base
titration, a ＼_____ shaped curve exists. From the facts that nitric
acid and sodium hydroxide are strong acid and strong base, respec-
tively, and that aqueous uranyl nitrate is a weak base, a titration
of a nitric acid-uranyl nitrate solution using sodium hydroxide gives
a ＼_____／ shaped curve.

A conductivity cell is used to measure the resistance (or con-
ductance) of a solution. There are many different types of cells,
but all consist of two separated electrodes. With fixed geometry,
the specific conductance, K_o, of a solution is:

$$K_o = \frac{1}{R_o A}$$

where R_o is the cell resistance, A is the cell electrode area and 1
is the distance between the electrodes. The ratio of A to 1 is often

termed the cell constant. The cell constant need not be known for
conductiometric titrations as long as it is constant throughout the
titration.

The resistance of a conductivity cell is usually measured by
means of an impedance bridge. An AC current source is normally used
in order to avoid polarization or reaction in the solution. Head-
phones, oscilloscopes, or AC nullmeters are usually used to determine
the balance point of the bridge.
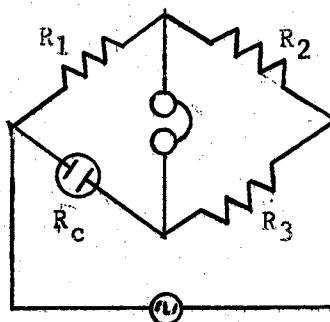
Impedance Bridge

When the bridge is balanced, the following relationship holds:

$$R_c = \frac{R_1}{R_2} R_3$$

The variable capacitor is used to balance out any cell
capacitance that may distort the determination of the null point.

The bridge circuit used to measure conductivity of the solution
being titrated consisted of an audio frequency (1 Kc) oscillator,
model 70029, Central Scientific Co., Chicago, Ill.; a Leeds &
Northrup Co., Student's Potentiometer, No. 7651; a Leeds & Northrup
Co. decade resistance box, model 245486; a decade capacitor, General

Radio Company, type 1419-K serial 666; and a set of high impedance headphones, A.M.D., No. 85-260.

The circuit used was similar to the circuit described earlier; with the slide wire in the potentiometer used as R_1 and R_2.

The conductivity cell was made from a 250 ml. Pyrex flask in which two electrodes of area one cm. were fixed about one cm. apart. The electrodes were embedded in glass tubing in which mercury was used as an electrical contact medium.

The acid titrations gave a mean selected normality of 1.056 N with a deviation of 0.2 per cent. This compares to the average selected mean normality of 1.058 N for the acid-uranyl nitrate (deviation of 0.3 per cent).

The complexing molar ratio of base to uranyl nitrate was found to be 2.319. Mundy (17) reported a complexing ratio of 2.305. It should be noted that this is not an accurate analysis for the uranium concentration. Poor results for the uranium concentration is due to the hydroxide precipitate which is formed upon addition of excess base. This precipitate causes poor conductivity measurements.

APPENDIX E

APPENDIX E

Numerical Solution to Fick's Second Law

In order to solve Fick's Second Law with the diffusion coeffi-
cient as a function of concentration, the numerical method of suc-
cessive approximations was used. The equation to be solved is

$$\frac{\partial C}{\partial t} = \frac{\partial}{\partial x}\left[D(C)\frac{\partial C}{\partial x}\right]$$

(E-1)

with

$$C = C_o, \qquad x < L, \qquad t < 0$$

$$C = 0, \qquad x > L, \qquad \text{all } t$$

$$\frac{\partial C}{\partial x} = 0, \qquad x = 0, \qquad \text{all } t$$

where L is the capillary length and x = 0 is the closed end of the
capillary tube. D(C) is approximated by the equation

$$D(C) = D_o + B\sqrt{C} + EC + FC^2 + GC^3$$

(E-2)

Perform the indicated operation on (E-1)

$$\frac{\partial C}{\partial t} = \frac{\partial D(C)}{\partial x}\frac{\partial C}{\partial x} + D(C)\frac{\partial^2 C}{\partial x^2}$$

(E-3)

when D = f(C) and C = f'(x,t)

$$\frac{\partial D}{\partial x} = \frac{\partial D}{\partial C}\frac{\partial C}{\partial x}$$

(E-4)

77

Substituting (E-4) into (E-3) yields

$$\frac{\partial c}{\partial t} = \frac{\partial D(C)}{\partial C} \left(\frac{\partial c}{\partial x}\right)^2 + D(C) \frac{\partial^2 c}{\partial x^2} \qquad (E-5)$$

The difference equations are

$$\frac{\partial c}{\partial t} = \frac{C_{i,j+1} - C_{i,j}}{\Delta T} \qquad (E-6)$$

$$\left(\frac{\partial c}{\partial x}\right)^2 = \left(\frac{C_{i+1,j} - C_{i-1,j}}{2\Delta x}\right)^2 = \frac{C_{i+1,j}^2 - 2C_{i+1,j}C_{i-1,j} + C_{i-1,j}^2}{4(\Delta x)^2} \qquad (E-7)$$

$$\frac{\partial^2 c}{\partial x^2} = \frac{C_{i+1,j} - 2C_{i,j} + C_{i-1,j}}{(\Delta x)^2} \qquad (E-8)$$

and

$$\frac{\partial D(C)}{\partial C} = \frac{B}{2\sqrt{C}} + E + 2FC + 3GC^2 \qquad (E-9)$$

Substituting Equations (E-6), (E-7), (E-8), and (E-9) into Equation (E-5) gives the forward difference expression.

The convergence criteria require that the coefficient of $C_{i,j}$ be positive. Therefore, collecting coefficients of $C_{i,j}$

$$\left[1 - 2\frac{D(C)\Delta T}{(\Delta x)^2}\right] > 0$$

or

$$\frac{\Delta T}{(\Delta x)^2} = \frac{F}{2D(C)} \qquad (E-10)$$

where $F > 1$

The forward difference expression was programmed and run on the IBM 360/50. Convergence was essentially attained with ten increments in the x variable. The program is presented on page 80.

```
//WPM1    JOB 12507-40074,10*,'METZ'
// EXEC FORTGCLG,TIME.GO=10
//FORT.SYSIN DD *
 99 FORMAT)10F10.7*
 98 FORMAT )10F10.2*
    DIMENSION C)1001,2*
    A=10.211E-06
    B=-16.61E-06
    E=28.561E-06
    F=-9.13037E-06
    G=-11.74E-06
    A=  8.738E-06
    B=-24.463E-06
    E= 39.566E-06
    F= 17.857E-06
    G=  3.550E-06
    P=0.5
    Q=1.0
    R=2.0
    S=3.0
 62 CONTINUE
    READ )5,99* CO, CAPL, TIME
C  L1 IS THE NUMBER OF POINTS IN TINE GRID
C  L2 IS THE NUMBER OF POINTS IN DISTANCE GRID
C STABILITY CRITERION IS DT/DX**2=F /2*D*  , F GREATER THAN 1.0
    L2=30
    L2=40
    L2=50
    L2=20
    L2=5
    L2=10
    L2=25
    AL2=L2
    FACT=5.0
    FACT=2.0
    FACT=1.
    AL1=TIME*2.0*A*FACT*AL2**2/)CAPL**2*
    L1=AL1
    AL1=L1
    WRITE )6,98* AL1, AL2
    T=TIME
    DX= CAPL/AL2
    DT=T/AL1
    DO 69 I=1,L2
    C)I,1**=CO
 69 CONTINUE
    LL=L2.1
 68 CONTINUE
    AJ = 0.
    DO 67 JJ=1,L1
    J=1
    C)LL,J**=0.0
```

```
    DO 66 I=1,L2
    IF )C)I,J** 57,57,56
 56 CONTINUE
    TERM1=A.. B*C)I,J***P .E *C)I,J***Q . F*C)I,J***R. G*C)I,J***S
    TERM2= P* B*C)I,J***)P-1* . E*G*C)I,J***)G-1* .F *R*C)I,J***)R-1*
 1.G *S*C)I,J***)S-1*
    GO TO 55
 54 CONTINUE
 57 CONTINUE
    TERM1=A
    TERM2=B
 55 CONTINUE
    IP=I.1
    IM=I-1
    IF)IM* 58,58,59
 58 CONTINUE
    IM=IP
 59 CONTINUE
    TERM3= )C)IP,J***2 -2*C)IP,J**C)IM,J*.C)IM,J***2*/4.0
    TERM4=C)IP,J*-2*C)I,J* .C)IM,J*
    TERM5= C)I,J*
    JP=J.1
    C)I,JP**=)TERM1*TERM4.TERM3*TERM2**DT/DX**2 .TERM5
 66 CONTINUE
    AJ = AJ . 1.
    TJME=TIME*AJ/AL1
    WRITE )6,99* )C)I,J*,I=1,L2*
    WRITE )6,98*   TJME
    DO 63 I=1,L2
    C)I,1**=C)I,2*
 63 CONTINUE
 67 CONTINUE
 65 CONTINUE
    SUM=0.0
    DO 64 I=1,L2
    IP=I.1
    SUM=SUM.)C)I,1*. C)IP,1***DX/2.0
 64 CONTINUE
    CBAR=SUM/CAPL
    CEND=CBAR/CO
    WRITE )6,99* CBAR
    WRITE )6,99*CO, CEND, CAPL, TIME ,AL1, AL2
    GO TO 62
 61 CONTINUE
    STOP
    END
//GO.SYSIN DD *
.05       2.0559      144000.
.25       2.0538      144000.
//
```

APPENDIX F

APPENDIX F

NOMENCLATURE

B = general parametric constant, Equation (5-4)

C = concentration, moles/liter

D = diffusion coefficient, $cm^2 sec^{-1}$

E = constant

ε = dielectric constant of a solution

F = constant

G = constant

H = distance of fringe deflection from base line, cm

h = hydration number

J_K = mass flux, moles $sec^{-1} cm^{-2}$

K = constant

M = molar concentration

n = refractive index

P = constant

Q = constant

R = refractive index increment, liter/mole

S = variance

$\mathcal{S}$ = slope of Nernst limiting equation

s = integer

t = time, sec

V = volume, liters

x = distance of fringe from refractive index gradient centroid, cm

x' = distance of fringe from an arbitrary center point, cm

y = general dependent variable

Greek Symbols

α = degree of dissociation

γ = ionic activity coefficient

Δ = difference

Δ_i = electrophoretic correction, $cm^2 sec^{-1}$

λ = equivalent conductivity, ohm^{-1}

η = viscosity, poise

ν = number of ions

σ = standard deviation

$\sigma_{\pm}$ = constant

φ = thermodynamic correction factor

Subscripts

a = phase A

b = phase B

i = component i

j = component j

o = limiting value

Superscripts

‾ = average

o = limiting value

1 = thermodynamically corrected

t = time corrected

VITA

William Patrick Metz

Candidate for the Degree of

Master of Science

Thesis: BIREFRINGENT INTERFEROMETER DIFFUSION MEASUREMENTS IN THE
URANYL NITRATE-WATER SYSTEM

Major Field: Chemical Engineering

Biographical:

Personal Data: Born in Keokuk, Iowa, June 4, 1945, the son
of Michael Joseph and Mildred Caroline Metz. Married
Karen Sue Peterson, August 28, 1965.

Education: Attended grade school in Keokuk, Iowa, and
Burlington, Iowa; graduated from Bear River High School,
Tremonton, Utah, in 1963; received the Bachelor of
Science Degree from Iowa State University of Science and
Technology, with a major in Chemical Engineering, in May,
1967; completed requirements for the Master of Science
Degree in May, 1969.